JPRS-CST-91-017
5 AUGUST 1991

Foreign Broadcast Information Service 50 ANNIVERSARY 1941 - 1991

JPRS Report

Science & Technology

China

Science & Technology
China

JPRS-CST-91-017 5 August 1991

CONTENTS

SUPERCONDUCTIVITY

TELECOMMUNICATIONS R&D

PHYSICS

Cryogenic Technology Used in Nation's Space Program Reviewed

91FE0608 Beijing WULI [PHYSICS] in Chinese Vol 20, No 3, Mar 91 pp 141-145

[Article by Zhu Senyuan [2612 2773 0337] of the Liquid Rocket Engine Institute, Beijing 100076]

[Text] Abstract: This article provides a brief outline of successful applications of cryogenic technology in China's space program: cryogenic technology in high-performance liquid hydrogen and liquid oxygen rocket propulsion systems, especially several key technologies in liquid hydrogen and liquid oxygen rocket engines. It describes some cryogenic technology and several miniature refrigerators used in space simulation experiment equipment for artificial satellites.

Cryogenic technology has already been rather widely used in China's space program, in these two main areas at present:

1. The use of high-performance liquid hydrogen and liquid oxygen rocket engines as primary power plants in liquid carrier rockets, which has promoted the development of several cryogenic technologies.

2. The development of artificial satellites requires outer space environment simulation experiments, and outer space is a cold and dark ultra-high vacuum environment with a temperature below 3 to 4K and an absorption coefficient of nearly 1. Satellites must be tested in equipment on the ground which can simulate this cold and dark small cosmic environment. It is apparent that the development of space flight technology requires the application of many types of cryogenic technology and also promotes further development of cryogenic technology.

I. Liquid Hydrogen and Liquid Oxygen Rocket Engines Have Promoted the Development of Cryogenic Technology in China

Liquid hydrogen is the fuel with the highest energy among chemical propellants. It has a very low density (70kg/m^3). A ball of liquid hydrogen the size of a ping pong ball would weigh about the same as a ping pong ball. Low temperature conditions of 20K (-253°C) are required to maintain hydrogen in a liquid state at one atmosphere. Thus, during the early stages when cryogenic technology was not highly developed, people had the mistaken notion that hydrogen was an absolute gas that could not be liquefied. It took 60 years from the time that liquid hydrogen was first obtained in the laboratory in 1898 until the United States first began developing liquid hydrogen and liquid oxygen rocket engines in 1958. The reason was that using liquid hydrogen as a fuel required both 20K cryogenic conditions and the establishment of a series of matching technologies like high-pressure liquid hydrogen transmission systems, various types of special materials for use in liquid hydrogen, various types of cryogenic measurement and metering systems, industrial production of liquid hydrogen and long-term storage, long-distance shipping, safe handling, and other projects. The development of engineering technology was carried out by levels. For example, production, storage, and long-distance transportation of liquid hydrogen required the development of vacuum insulation technology, various types of cryogenic sealing technology, and the formulation of technical safety conditions and operation conditions for safe transport of liquid hydrogen on railroads and highways. Developing liquid hydrogen and liquid oxygen rocket engines also required development of liquid hydrogen and liquid oxygen combustion technology, liquid hydrogen pump and liquid hydrogen valve design theory, liquid hydrogen supply system flow rate control technology, cryogenic high-speed bearings, special cryogenic operation, static sealing, and large power transmission cryogenic high-speed gears, and so on. Thus, using liquid hydrogen as an industrial fuel required the establishment of a complete and matching cryogenic technical foundation and the corresponding facilities.

In accordance with a proposal by Qian Xuesen [6929 1331 2773], China began exploring the use of liquid hydrogen in rockets in 1964, but shortly afterward the decade of chaos in the "Great Cultural Revolution" began and this work stopped completely. In 1970, following China's first successful launch of an artificial satellite, to further develop China's space flight industry and in response to proposals by Qian Xuesen and Ren Xinmin [0117 2450 3046], experimental research on the use of liquid hydrogen in rockets was resumed. By this time, the United States had successfully used liquid hydrogen and liquid oxygen rocket engines in its "Centaur" rockets and "Apollo" program and France had been engaged in experimental research on small-thrust liquid hydrogen and liquid oxygen rocket engines for 6 or 7 years. China's research on liquid hydrogen and liquid oxygen rocket engines actually began rather late and in a situation of a poor cryogenic technology foundation. China had to establish its own liquid hydrogen cryogenic technology during the process of developing liquid hydrogen and liquid oxygen rocket engines, which greatly increased the complexity of developing liquid hydrogen and liquid oxygen rocket engines. We will now introduce several typical liquid hydrogen cryogenic technologies.

A. The question of safe discharge of cryogenic hydrogen[1]

The problem of discharging cryogenic media (liquid nitrogen, liquid oxygen, or their cryogenic gases) is very simple since all can be discharged directly into the atmosphere. There are special requirements, however, for discharging liquid hydrogen or its gas. After a liquid hydrogen storage tank functions, the residual cryogenic hydrogen must be discharged, which requires special attention to fires, explosions, and other safety questions.

When hydrogen gas is flowing at high speeds or dual-phase hydrogen flows in a discharge pipe, it can generate a very high electrostatic potential difference. We measured an electrostatic potential difference of 8,000 V to 12,000 V at a hydrogen discharge outlet. It is very easy for the direct discharge of a hydrogen gas flow with this high potential into the atmosphere to cause fires or explosions. Actual measurements have shown that the potential difference in the hydrogen gas flow is related to the velocity of the gas flow as well as to the gas-to-liquid ratio, the temperature of the gas flow, and other factors. This means that the potential difference of the discharged hydrogen gas flow is related to the Mach number of the gas flow, so restricting the Mach number of the gas flow within a certain safe range can enable the safe discharge of hydrogen gas. After gaining an understanding of the characteristics of hydrogen discharge, we had to formulate several handling regulations, so the technology involved in using hydrogen as an industrial fuel is actually not complicated. We have safely transported large amounts of liquid hydrogen by rail and highway without a major accident.

B. High-speed liquid hydrogen ball bearings

High-speed liquid hydrogen ball bearings have these characteristics compared to regular high-speed bearings:

1. Because the viscosity of liquid hydrogen is very low, fluid dynamics lubricating film theory cannot be used to lubricate liquid hydrogen bearings. Another method of lubrication is required.

2. Because liquid hydrogen bearings are produced and installed under normal temperatures, suitable gaps must be left when designing liquid hydrogen bearings for cryogenic operation to prevent them from seizing due to cryogenic contraction during operation.

3. Under cryogenic conditions, there is contact stress between the balls and races, the effects of which can cause phase transformation in austenic bearing steel and turn it into martensite steel, which involves a process of crystal lattice enlargement. Thus, gap designs that only take temperature shrinkage into consideration cannot ensure reliable operation of liquid hydrogen bearings. Special cryogenic processing is required for the bearing steel.

4. The "Dn" value of ball bearings is usually used to describe their working conditions because bearing life is related to their "Dn" value. D here is the bearing diameter (mm) and n is the working revolutions per minute. Reference [2] states that high-speed bearings have a "Dn" value equal to or greater than 600,000 while ultra-high speed bearings have a "Dn" value greater than 1 million. Nearly all bearings in liquid hydrogen pumps are ultra-high speed bearings and many bearing breakdowns are related to the quality of their cooling. When ultra-high speed bearings are operating, the inner and outer races generate large amounts of heat, but heat output is most severe in the inner race. The cooling should be focused on the inner race. This question must be guaranteed in the design of the holder. Lubrication of liquid hydrogen bearings as mentioned previously also means relying on self- lubrication of the holder material, which means that the material and structure of the holder are extremely important questions.

The holder is a porous circular thing. When the bearing is operating, it can ensure that the balls do not collide, but the balls can come into contact with the holder. When the balls are spinning at high speeds, they are also being turned along with the holder. Holder materials which have self-lubricating properties are continually worn by the balls. A thin layer of lubricant adheres to the surface of the balls themselves to lubricate the liquid hydrogen bearings. Because the spin rate of the balls is very high and their inertial force is also large, no collision of any sort can be permitted. Thus, when the holder is turning along with the bearings, there must be a guide surface. Those with an outer ring guide are called outer ring holders. Those with an inner ring guide are call inner ring holders. There is still debate over which type of holder to use in the design of liquid hydrogen bearings. Reference [2] states very clearly, however, that theory and practical experience both show that using outer guide holders for liquid hydrogen bearings conforms to requirements. Nearly all the liquid hydrogen bearings developed in the United States are outer guide holders. Liquid hydrogen bearings are a new technology and much more work requires study and improvement.

C. Sealing technology for liquid hydrogen work

Seals used on liquid hydrogen and liquid oxygen rocket engines can be divided into two categories, static seals and active seals. Seals working under liquid oxygen conditions are relatively easy to deal with. Because the viscosity of liquid hydrogen is very small, about 14 times less than liquid oxygen, the molecular weight of hydrogen is also the smallest. Therefore, the sealing technology for use in liquid hydrogen is relatively complex.

1. Static seals, which are seals connecting various assemblies, conduits, and so on. Because the materials of the various connecting components are not necessarily identical, their shrinkage coefficients are also different. When engines are operating, they are affected by pre-cooling, startup, shutdown, repeated pre-cooling, repeated startup, and other alternating temperature changes and working vibrations as well as other factors which make reliable operation of seals difficult. The following principles should be adhered to in dealing with this type of seal. First, there should be concern for using temperature stress to help improve the seal during cryogenic operation. Second, the materials used in cryogenic seals must be rationally selected. Because almost all non-metallic seals become brittle at liquid hydrogen temperatures and can even "turn to glass", this problem must be solved by using composite materials.

2. Active seals. There are many different forms of active seals in liquid oxygen engines. The most technically

difficult are the end seals on the high- speed axles of hydrogen and oxygen turbine pumps. They are located on the high-speed axle where there is high-pressure liquid oxygen at one end and cryogenic hydrogen at the other end, or there may be high-pressure liquid hydrogen at one end and high-temperature burning gas containing a steam component. Active seals which function under such terrible conditions cannot function as absolute seals, nor it is necessary that they do. In a certain sense, sealing technology is actually leakage rate control technology, a technology that controls the leakage rate within a permissible range. Thus, stipulation of a rational leakage rate can permit safe utilization and the problem is easily solved. NASA in the United States has stipulated that an absolute sealing requirement is a seal in which the leakage rate does not exceed 1 $cm^3/a/in$ at a pressure difference of 1 atmosphere (in an air medium)[3]. In engineering, a zero leakage rate is stipulated as a seal of 3.171 X $10^{-8}cm^3/s/in$. We can set different permissible leakage rate values according to different application conditions and the sealing problem is simplified. The active seal design for the end of a cryogenic high-speed axle first requires rational selection of operating parameters. Important parameters include the working pressure difference (4p) ahead of and behind the seal, the rotation speed of the axles, or the tangential velocity (v) of a pair of friction surfaces. Here, the product Δ p X v is an important parameter affecting the lifespan of the end seals. This value should be chosen as small as possible. The second is the need to select an optimum friction surface combination. If the materials are poorly matched, meaning that the seal has a small Δ p X v value, the lifespan will also be short. The third thing is to ensure a small friction coefficient on the friction surfaces. Hydrogen has very poor lubrication properties, so the materials must be self-lubricating. The biggest problem is changes in friction coefficients during the operation process which lead to instability in seal operation and even cause vibration and destruction of the seal. Thus, the main thing involved in the end seals of high-speed axles is a great deal of arduous experimentation to obtain a rational solution to the problem.

D. Cryogenic high-speed drive gears

When a rocket engine ceases operating, the desire is to have the least amount of propellant remain in the rocket tank. This requires strict control of the rotation speed of hydrogen pumps and oxygen pumps to make them operate at the stipulated rotation speed ratio. Using gear drives to achieve the stipulated rotation speed ratio for the two pumps is a relatively simple method on small-thrust engines. Because of the low density of liquid hydrogen, liquid hydrogen pumps must operate at high speeds but liquid oxygen pumps should not rotate at too high a speed. This requires a high-speed cryogenic drive gear. The problems in designing a high-speed cryogenic drive gear device are:

1. The lubrication problem of high-speed cryogenic drive gears. Lubrication here is different from ball bearings. When the gears are functioning, there is both rolling and sliding friction on the surface of the gears. There is a positive relationship between the heat output of the gear surface and the drive power of the gear. Using a solid lubricating film requires that the lubrication film material have cryogenic ductility, be strongly bonded to the gear steel, and have a linear expansion coefficient that is basically near that of the gear steel.

2. The problem of controlling gear heat output. The heat output of the gear is mainly related to the amount of sliding friction on the gear surface. A small modulus gear can reduce the sliding friction on the gear surface.

3. The problem of preventing temperature deformation of the gear box casing. High-speed drive gears demand very high meshing precision. However, the gear box casings of hydrogen and oxygen pumps cannot guarantee a homogeneous temperature field. The temperature difference between liquid oxygen and liquid hydrogen can be as much as 70K and the temperature difference between a liquid hydrogen pump and a gas-fired turbine on the same axle can be 900K. The temperature difference at insulated locations is approximately the same as that between the liquid hydrogen and liquid oxygen and there is severe heating of some locations by liquified air. Temperature deformation of the gear box casing can prevent guarantees of parallelism between the two axles which can reduce the precision of the meshing of the gears or create offset friction. This requires adoption of several measures like reducing temperature deformation, changing the shape of the gears, and other complex operations.

E. The problem of flow rate measurement in cryogenic media

Launching a communications satellite into geosynchronous orbit places even higher demands on the amount of rocket engine propellant consumed per second and the desire is to have a minimum amount of propellant remain in the tanks when the engines shut down. This requires an increased precision of flow rate measurement in the cryogenic medium. High-precision flow rate measurement systems with three different working principles have been established during liquid oxygen engine development.

1. A high-precision graded capacitance liquid level indicator and microwave resonant cavity densitometer are installed, respectively, in the insulated liquid hydrogen and liquid oxygen tanks to form a mass flow rate measurement system that can measure the average flow rate during the process of engine operation.

2. Turbine flowmeters and coaxial capacitance densitometers are installed in the pipelines to form another mass flow rate measurement system that can measure the average global flow rate and transient mass flow rates during the process of engine startup and shutdown.

3. Using a dynamic weighing method. The liquid hydrogen and liquid oxygen flowing out of the tanks during the process of engine testing are weighed and

divided by the time interval to obtain the mass flow rate. This principle is very simple but many problems are involved in using it. There are many conduits connected to the cryogenic insulated tanks and all sorts of temperature stresses affect the tank system. Vibration passing through the conduits and base during engine testing affect the precision of the measurement system. However, by adopting effective vibration damping measures and scientifically "peeled" weighing, this is an extremely reliable high-precision cryogenic flow rate measurement system.

By independently carrying out precision correcting and error analysis and comparing these three systems, the measurement results are extremely reliable.

This shows that development of hydrogen and oxygen engines has promoted the development of many cryogenic technologies and formed a new technical realm. This new technical realm is playing an important role in China's four modernizations drive. The third stage of China's Long March-3 carrier rocket is a high-performance liquid hydrogen and liquid oxygen rocket. It has successfully launched six geosynchronous communications satellites since 1984, including the Asia-1 communications satellite (manufactured by the Hughes Corporation in the United States) on 7 Apr 90 that successfully provided communications for China's Asia Games. China is now continuing to develop even better hydrogen and oxygen rocket technology to further improve the performance of Chinese carrier rockets.

Liquid hydrogen is a high-performance chemical fuel as well as the cleanest fuel. The product of its combustion with oxygen is water vapor, which causes no pollution of the environment and does not emit large amounts of CO_2 like the combustion products of petroleum products which raise global atmospheric temperatures. When we begin widely using liquid hydrogen fuel, we can achieve benevolent cycles in the natural environment and basically protect the global environment on which mankind depends for its existence.

The United States has made a preliminary decision to use advanced launch systems and space-ground travel transport systems in the 21st Century which will all use liquid hydrogen as a fuel. Japan and Western Europe are now developing 100-ton thrust grade large hydrogen and oxygen rocket engines that are expected to be put into use in the mid or late 1990's. Nations of the world with advanced space flight technology are thinking about developing liquid hydrogen-fueled air breathing space flight engines. It is apparent that continual expansion of the scope of liquid hydrogen applications has become an inevitable development trend. The 21st Century will be an era in which cryogenic technology engineers can make great accomplishments.

II. Space Simulation Equipment and Miniature Refrigeration Equipment

Development of satellite engineering must be based on matching space environment simulation experimental equipment. This type of equipment is usually large vacuum tanks with a solar simulator inside and a cold and dark wall lining on the walls of the tanks called a heat sink. If there is an extremely high vacuum in the tank, the vacuum of satellite operation orbits can be basically approximated. The temperature of the heat sink wall lining can be reduced to 3 to 4K, so it is entirely capable of simulating space conditions. However, the technical difficulty involved in establishing this type of equipment is too great and it is unnecessary. Although it can create definite errors, using theoretical analysis and experimental confirmation to make simple environmental simulation equipment can greatly reduce experiment and equipment costs, and these errors do not affect engineering applications. For example, if the surface temperature of a spacecraft is 300 to 350K, the heat sink wall layer temperature required to simulate the cold and dark conditions of space when doing experiments in an environmental simulator only has to reach 100K, and the induced error at this temperature is only 1 percent greater than the error induced by actual space temperatures. This is permissible. Thus, many experiments can be conducted in liquid nitrogen process simulators, so expensive liquid hydrogen processes are not needed. This can reduce equipment operating costs and satellite experiment costs.

China has established several space environment simulators since 1964. I will now provide a brief introduction to some representative space simulation equipment.

1. KM-3 simulator. This simulator was completed in 1970 and is used as space environment simulation equipment for full-unit satellite tests. The container is 3.6 m in diameter and 7.3 m long. There is a copper liquid nitrogen heat sink inside the container which has a liner wall temperature of 90K and a heat absorption coefficient of 0.93. To increase the experimental vacuum, the KM-3 has a cooled helium wall liner (the temperature is below 20K) and the ultimate vacuum is 5.6×10^{-7} Pa. Later, a cold helium heat sink below 20K will be added in the container. Helium turbo-expander cooling is used in the cold helium process, which increased the experimental capacity of the equipment.

2. KM-4 simulator. This simulator was completed in 1978 and was built to carry out full-unit space environment simulation experiments for geosynchronous satellites. The container is 7 m in diameter and 12 m high. Its ultimate vacuum is 1×10^{-6} Pa and its heat absorption coefficient is 0.92. A copper liquid nitrogen heat sink is installed inside the container and it has a cold helium wall liner heat sink with an extraction speed of 2×10^{6} l/s and a temperature as low as 16 to 18K. The outer process of the cold helium wall plate is a Braden cycle that has a turbo-expander. The turbine rotation speed is 88,000 rpm and the cooling power at 20K is 1,200W. During actual operation, the intake temperature of the turbo-expander is 16K, the exhaust temperature is 11K, and the temperature of the helium-cooled wall liner is below 15K.

A single-phase closed cycle liquid nitrogen process is used for the heat sink outer contact cryogenic process in the KM-3 and KM-4. After the liquid nitrogen circulating in the pipes receives its full heat load, it still maintains a single-phase subcooled state. There are no evaporation losses of the liquid nitrogen in the pipes. Boiling and consumption of the liquid nitrogen only occurs outside of the subcooler circulation pipes. China has several pieces of space environmental simulation equipment that use this process. Their operation is stable, they have good heat sink temperature homogeneity, they have a strong capacity for bearing unevenly distributed loads, and the precision of the simulation experiments can be maintained throughout their operation.

China has also made progress in space refrigerators and miniature refrigerators. We began preparatory research on space cooling technology in the 1960's. The main development projects at that time were: radiation cooling, solid cooling, miniature flow regulation cooling, and mechanical refrigerators for use in space. I will now describe some representative products.

During the 1970's, China developed the "two-stage Solvay refrigerator" and "two-stage Gifford-McMahon refrigerator". The ultimate cooling temperature was 9K. Their cooling capacity at 20K was 5 W to 10 W. This refrigerator was used in a cooling parameter amplifier for a communications satellite ground receiving station. It is now used mainly in cryogenic vacuum pumps.

China successfully used radiation refrigerators on its FY-1 [Fengyun-1] meteorological satellite. This two-stage radiation refrigerator can attain a low temperature of 105K and is used in cooling HgCdTe infrared detectors.

Solid argon refrigerators that may be used on satellites are now being developed. We are also studying Vuilleumier refrigerators and we have employed magnetic drive technology in 2 W single-stage water coolers and 3 W single-stage air coolers and refrigerators with temperatures as low as 77K. We have successfully developed on-board Stirling refrigerators (0.5 W, 35K), and we are developing rhombohedral drive dual-stage Stirling refrigerators with minimum temperatures of 26K.

China has just begun applying cryogenic technology in its space program. The scope of applications is now expanding and we should extend cryogenic power into our aviation program in the future. Liquid hydrogen is a high- performance and clean fuel and we should use it in aviation engines as soon as possible and even in automobile engines. Several scientifically developed western nations are now doing experimental research on using liquid hydrogen fuel in aviation engines and automobile engines. China should begin research soon. I believe that in the not-too-distant future, cryogenic technology will have even broader applications prospects.

References

[1] Zhu Senyuan [2612 2773 0337], DIWEN GONGCHENG (CRYOGENIC ENGINEERING), No 2, 1979 p 55.

[2] Leo W. Winn, NASA CR-134615, 1974.

[3] D. K. Huzel et al., NASA SP-125, 1967 p 321.

LM-4 Two-Way Swivelling Servomechanism Detailed

91FE0607B Beijing SHIJIE DAODAN YU HANGTIAN [MISSILES & SPACECRAFT] in Chinese No 4, 20 Apr 91 pp 33-35

[Article by Zheng Shizhuang [6774 0099 1104], senior engineer in Xinyue Instruments Plant, Shanghai Space Bureau: "Two-Way Swivelling Servomechanism"]

[Text] Abstract: A Long March-4 [LM-4] carrier rocket launched the first Fengyun-1 meteorological satellite from the Taiyuan Satellite Launch Center on 7 Sep 88 with gratifying success. The third substage of this rocket used a two-way swivelling servomechanism for the first time in the history of Chinese carrier rockets. This article describes the development situation, composition, principles, and primary technical indices of this servomechanism.

Key terms: thrust vector control system, positioning servomechanism, carrier rocket, China.

I. Outline

A rocket thrust vector control system is a typical electrohydraulic positioning servo system that has stationary movement, fast response, large power, simple actuation components, and other advantages, so it is widely used in missiles and spacecraft.

All of China's large carrier rockets use electrohydraulic positioning servomechanisms. They have four liquid rocket engines, each swinging in a single direction for thrust vector control, thereby achieving rocket pitching, yawing, and rolling attitude control and stabilization. The third substage of the LM-4 carrier rocket used a YF-40 two-way swivelling engine for the first time which requires only two engines to achieve rocket attitude control and stabilization.

Work to develop the two-way swivelling servomechanism began in 1978. The first thing encountered at that time was the question of program selection. For electrohydraulic servomechanisms, the operational principles were the same regardless of the scheme adopted. Program selection mainly involved selection of the hydraulic energy system. These were the main oil pump drive schemes at that time:

1. Drainage (using the energy in the liquid engine);

2. Drainage + pressure storage vessel electromagnetic valve;

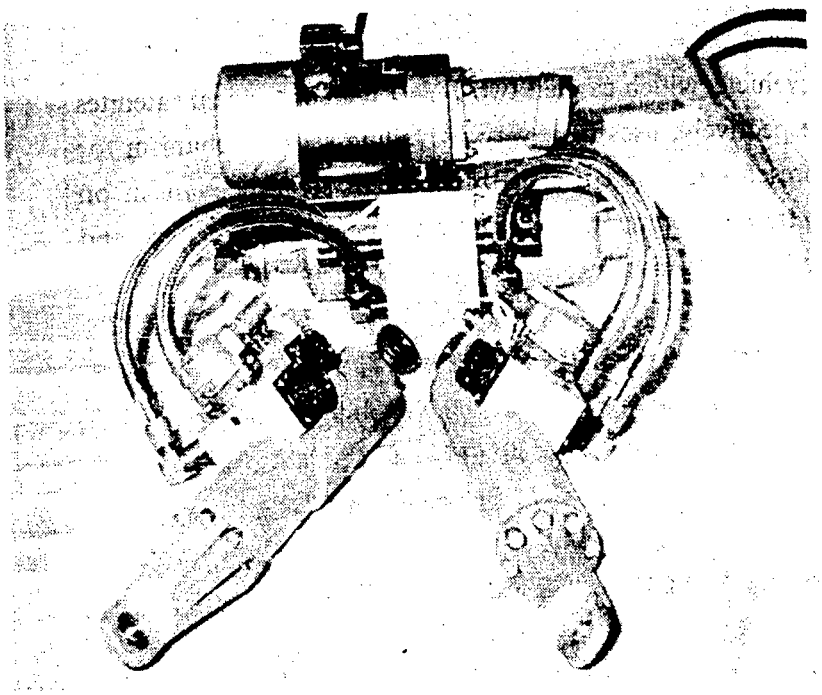

Figure 1. Exterior of Two-Way Swivelling Servomechanism

3. Drainage + auxiliary DC electric pump;

4. DC electric pump.

Based on the actual control targets of the LM-4, we selected a DC electric pump as the energy source system for the two-way swivelling servomechanism. The DC electric motor can be started up in advance to achieve cold swivelling and improve the initial control conditions. The DC electric pump scheme can take into account ground testing and eliminate an auxiliary oil pump system, so testing, application, and maintenance are convenient. The biggest advantage of this scheme is the small mass of the product. The mass of the servomechanism is just 20.5 kg.

II. Composition

The main components of the two-way swivelling servomechanism are an oil source assembly and two servo actuators. The oil source assembly provides motive power to the servo actuators. It is composed of DC electric motor, piston- type fixed displacement oil pump, sealed oil tank, piston-type pressure storage vessel, one-way valve, oil filter, overflow valve, high and low pressure safety valves, high and low pressure metallic hoses, and other hydraulic components.

The servo actuators convert the hydraulic force in the oil source assembly according to electrical signals into mechanical force on the thrust engines. They are composed of servo valves and actuators (valve-controlled oil cylinders), feedback potentiometers, automatic bypass valves, and other components. In addition, control, telemetry, electric motor, and other sockets are installed on the two-way swivelling servomechanism for use in transmitting the electrical signals.

Based on telemetry and ground testing requirements, a pressure storage vessel gas-filled pressure transducer, oil tank oil surface potentiometer, oil tank oil surface temperature transducer, and so on are also installed on the servomechanism. All of these things are linked together organically to form a sealed system after being filled with oil and gas. This increases product reliability and flexibility of use and operation. Figure 1 shows the exterior of the two-way swivelling servomechanism.

The hydraulic pump in the two-way swivelling servomechanism is a fixed displacement pump driven by an electric motor. After the hydraulic pump is started up, it draws in oil from the oil tank. After the high pressure oil it discharges passes through the oil filter, one-way valve, and magnetic oil filter, it is divided into three loops: the first loop passes through the high-pressure metallic hose and is transmitted to the two servo actuators, the second loop enters the pressure storage vessel, and the third loop passes through the overflow valve and returns to the oil tank.

When the servomechanism has not received a command signal input, the valve cores of the servo valves on the left and right servo actuators are in an intermediate position, the throttle aperture is closed, and the actuator piston rod is in the zero position to lock the engine.

When the servomechanism receives a command signal input, the servo valve throttle apertures of the left and right servo actuators are opened and the high-pressure

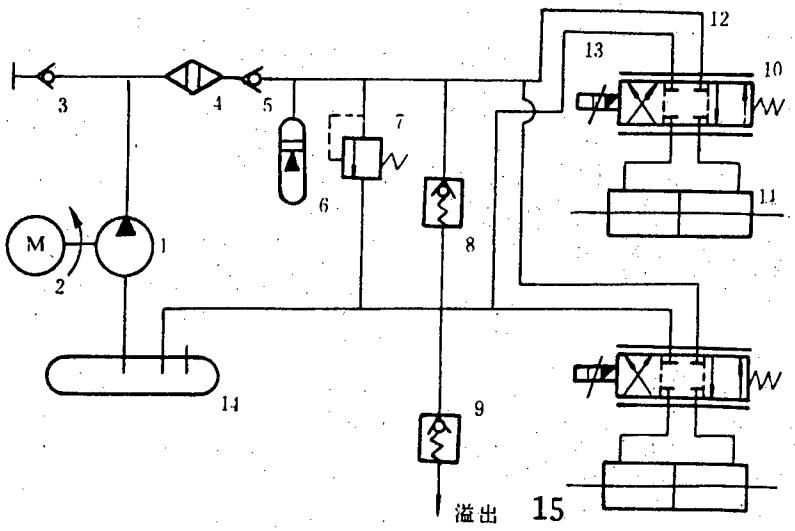

Figure 2. Diagram of Hydraulic Principles of Two-Way Swivelling Servomechanism

Key: 1. Oil pump 2. DC electric motor 3. High-pressure injection valve 4. Oil filter 5. One-way valve 6. Pressure storage vessel 7. High-pressure overflow valve 8. High-pressure safety valve 9. Low-pressure safety valve 10. Servo valve 11. Actuator 12. High-pressure metallic hose 13. Low-pressure metallic hose 14. Oil tank 15. Overflow

oil enters one chamber of the actuators, pushes the piston rods, and causes two-way swivelling of the engines. At the same time, the oil in the other chamber of the actuators passes through the other throttle aperture in the servo valves and returns to the oil tank via the low-pressure metallic hoses.

For safety reasons, safety valves used for overload protection are installed in the high and low-pressure return loops. Automatic bypass valves are installed on the actuators to open up the two chambers of the actuators and move the piston rods for installation of the servomechanisms.

The servomechanisms themselves can only function as an open loop, meaning that when the servomechanisms receive a current signal input, they output at a specific rate. When they are connected to the upper servomechanism amplifier and the output signal from the feedback potentiometer is fed back to the servo amplifier, the servomechanisms can be in a closed-loop operating state. This constitutes the positioning servo system that swings the engines.

III. Structural Properties

Two servomechanism schemes can be used to achieve two-way swivelling of the engines. One is an integral type in which each servo actuator is fitted with a hydraulic energy source and electric pumps are used for the energy source power. This structural arrangement requires two electric pumps, so the mass of the servomechanisms must be greater and the battery capacity required on the rocket is larger, so this was not chosen. The servomechanisms now used employ a dispersion scheme in which an energy source is connected through metallic hoses to the two servo actuators. This scheme has a tight structure and rational configuration. The configuration of the servomechanisms and engines is illustrated in Figure 3.

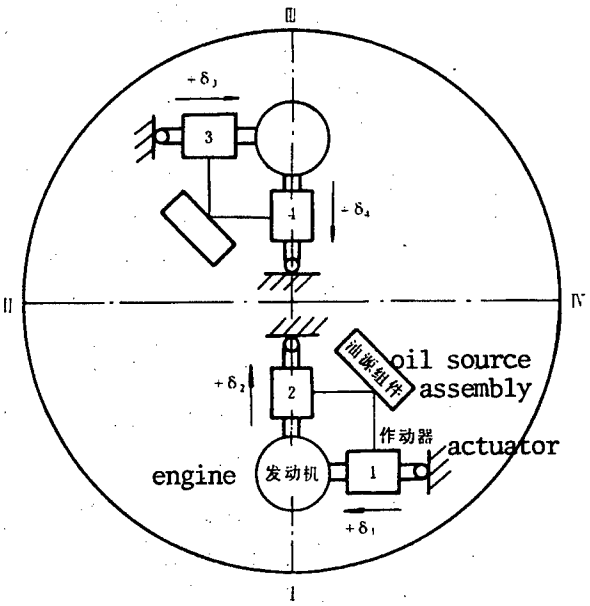

Figure 3. Configuration of Two-Way Swivelling Servomechanism and Engine

Automatic bypass valves are used for the two-way swivelling servomechanism bypass valves. This was also new in China. This structure is shown in Figure 4.

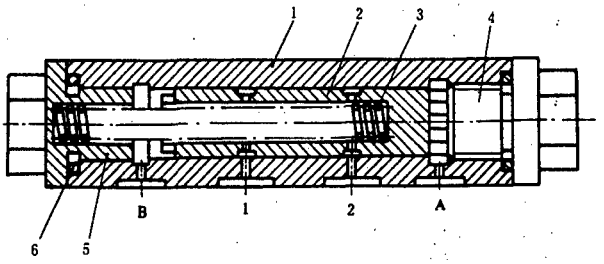

Figure 4. Structural Diagram of Automatic Bypass Valve

Key: 1. Valve body 2. Valve core 3. Spring 4. Plug 5. Plug 6. Sealing ring

The working principles of the bypass valves are: when the servomechanism begins to operate, pressure builds quickly in the servomechanism and oil is supplied to the servo valves. At the same time, the pressure increases in chamber A of the bypass valves. When the pressure reaches 1 MPa, the valve core end surface pressure spring balances the compressional force on the spring with the pressure on the end surface of the valve core and the valve core stops moving, cutting off chambers 1 and 2 of the actuator. When it stops, the restoration force of the spring (49.1N) is used to open up both chambers of the actuator.

The automatic bypass valves have a tight structure and are safe and reliable. Operation and maintenance is also very convenient.

IV. Servomechanism Performance

The main performance indices of the two-way swivelling servomechanism are:

Rated load moment of force	766.88 Nm
Output turn angle	+/- 4°
Output load angle speed	≥20°/s
Output empty load angle speed	≥38°/s
Maximum actuator thrust	7495 N
Electric motor current consumption	<52 A
Continuous operating time	15 min
Mass	20.5 kg

V. Conclusion

Gratifying success was achieved in China's first launch of a Fengyun-1 experimental meteorological satellite on a LM-4 carrier rocket from the Taiyuan Launch Center on 7 Sep 88. Subsequently, the September 1990 launch of Fengyun-1(B) was also successful. This confirms that the two-way swivelling servomechanism scheme used on the third substage of the LM-4 carrier rocket is feasible. We will also use this technology on China's other Long March rocket models in the future. Successful development of the two-way swivelling servomechanism fills in a blank space in China in this area.

ZN-3 Sounding Rocket Said Essential to Space Physical Studies, Manned Spaceflight

91FE0607A Beijing SHIJIE DAODAN YU HANGTIAN [MISSILES & SPACECRAFT] in Chinese No 4, 20 Apr 91 pp 16-17

[Article by Xiao Guangquan [5135 0342 0356] and Yang Junwen [2799 0193 2429] of the Chinese Academy of Sciences Space Science and Applied Research Center: "Launch Test of ZN-3 Sounding Rocket"]

[Text] Abstract: The Chinese Academy of Sciences Space Science and Applied Research Center [CAS SSARC] and other units successfully launched two ZN-3 [Zhinü—Vega] sounding rockets from the Hainan Sounding Rocket Launch Site in January 1991. They added 120 kilometers of sounding measures to China's rocket sounding system. The Hainan Large Rocket Launch Site provides an excellent location for China's space environment sounding and comprehensive observation of low-latitude regions.

Key terms: sounding rocket, atmospheric physics, spacecraft launch site, China.

Two ZN-3 sounding rockets were launched from the Hainan Sounding Rocket Launch Site on 21 Jan and 26 Jan 91. They were jointly developed by the CAS SSARC, China National Defense Science and Technology University, and the Changzheng [Long March] Machinery Plant and Jingwei Chemical Fiber Plant under the jurisdiction of Unit 620 in Jiangxi. The two rockets carried scientific nose cones to altitudes of 147 kilometers and 127 kilometers, respectively, for the CAS SSARC. The rocket telemetry and data processing systems, positioning system, attitude measurement system, and so on all provided the required data.

Sounding and research on the space environment are essential for development of the space industry and space science research. There are four main ways to do sounding of the space environment at present: satellites can do long-term large-area sounding at altitudes greater than 200 kilometers, scientific balloons can do sounding of atmospheric parameters below 40 kilometers over long distances and long periods, and various types of ground-based scientific equipment can make long-term indirect observations of space from fixed sites, but sounding rockets are the only means of direct sounding of space within an altitude range of 40 to 200 kilometers. Thus, they have received attention in all nations, especially in those countries which are developing space technology and doing space science research. About 20 nations like the United States, Soviet Union, Japan,

Germany, England, India, and so on have developed and applied sounding rocket systems at different altitudes for sounding and study of the middle and upper layers of the atmosphere, the ionosphere, the magnetosphere, the Sun, and so on. They have accumulated large amounts of space environment data that provides a wealth of information for space technology and space science research. Each of these four measures have their own characteristics and are mutually complementary, but none is a substitute for the others.

Launching large carrier vehicles and launching and recovering manned spacecraft both require real-time sounding of atmospheric parameters at about 120 kilometers and below. These are essential space parameters for guaranteeing flight safety. The new ZN-3 sounding rocket developed by China has achieved the expected objectives through major cooperation by S&T personnel in relevant units and several years of hard work. It has raised China's sounding rocket technology to a new level and can provide new and more perfect sounding systems for China's space sounding. Before this, China had already successfully developed the ZN-1 and Heping-6 [Peace-6] small meteorological rockets used at altitudes below 60 to 80 kilometers. This provides a practical space sounding system for the development of space technology, large carrier vehicle experiments, launch and application of manned aircraft, space science research, and other areas.

I. The ZN-3 Sounding Rocket

The ZN-3 sounding rocket system (see front cover) includes four parts: a rocket carrier; a scientific nose cone; a telemetry system, tracking radar, data processing system, and other ground-based equipment; and launch site facilities.

The ZN-3 rocket is a two-stage solid carrier rocket. The rocket has a total length of 4.87 meters and the total weight of the rocket is 285 kilograms. When the nose cone weighs 45 kg (the scientific instruments weigh 25 kg) and the launch inclination is 86°, the apex of the trajectory is 147 kilometers, and when the launch inclination is 83.9°, the apex of the trajectory is 127 kilometers, which enables sounding of the E-layer region of the ionosphere. This shows that in addition to China's ability to supply atmospheric rocket sounding systems, we have also added 120 kilometer altitude sounding measures for larger payloads.

The ZN-3 sounding rocket uses a multi-circuit telemetry system with a 400 MHz carrier frequency with three FM channels and one pulse-code (PCM) channel for transmitting scientific information at a code speed of 9.6 KBPS using a 64-circuit primary exchange and 32-circuit auxiliary exchange. When the telemetry transmitter on the rocket has a power of 1W, the telemetry transmission distance can be as much as 500 kilometers. An L-band radar responder measures the rocket's flight orbit and a flux gate tri-component magnetometer and solar angle meter measure the rocket's flight attitude.

II. Hainan Sounding Rocket Launch Site

An observation test launch site is required for space research, and this site must be capable of being used for rocket sounding as well as for ground-based observation and even for stratospheric balloon experiments. Internationally, there are already several such sites at moderate and high latitudes, but there are relatively few comprehensive rocket observation test sites in low-latitude regions near the equator, just a few tests sites in the United States, Brazil, India, and so on up to now. There are many international vanguard topics and applied and basic topics that await study in low-latitude regions, such as the effects of ionospheric anomalies on radio wave propagation in equatorial regions and the quality of remote sensing images, and so on, all of which are topics of universal concern internationally. After China completed the sounding rocket launch site on Hainan, the first successful launch of four ZN-1 meteorological rockets was done in December 1988 and we obtained atmospheric data below 60 kilometers.

Hainan Sounding Rocket Launch Site is located on the northwest coast of Hainan Province in the Fuke region 192 kilometers southwest of Haikou City at 19°30' north latitude and 109°8' east longitude. The elevation is 78 meters above sealevel and the launch site is about 18 kilometers from the coast. It is a comprehensive testing base area built and operated by the CAS SSARC and conducts space science sounding research in equatorial regions. The launch site region has a tropical monsoon climate and is an excellent site for studying the middle and upper atmosphere and ionosphere in equatorial regions. Equatorial regions are a key region for conducting space science sounding. Ionospheric phenomena are extremely abundant and one can frequently observe ionospheric inhomogeneous structures that are not easily observed at middle latitudes. A rocket matched with ground-based observation equipment may be able to obtain important research results.

Hainan Launch Site together with China's existing Mohe, Beijing, and Wuhan scientific observation stations form a chain of space observation stations. Simultaneous observations by multiple stations along a particular meridian can be used for research on many space physics topics.

The main equipment at the launch site includes the main experiment building, rocket assembly building (containing an electric-powered crane with a 1-ton lifting capacity and several laboratories), the launch ground, a flammable materials warehouse, a launch control bunker, power supply and matching equipment, the corresponding living facilities, and so on. Based on short-term sounding experiment requirements, the launch site is outfitted with a radio timing system, radio communications network, and radar data wire transmission system. All this equipment functioned normally during this launch test.

The launch ground is located about 1.7 kilometers west of the main building and about 200 meters from the launch control bunker. The rockets are launched slightly west of a northerly direction. The first stage drop area is sparsely populated and the second stage drop area is in the sea of Beibu Gulf.

A sounding rocket launch site is different from a satellite or large carrier vehicle launch site. For the former, launch windows are selected according to scientific research topics and the corresponding space phenomena like solar eruptions, solar eclipses, meteors, geomagnetic activity, and so on. As a result, the rocket launch facilities must be convenient and flexible and the rocket launch site must be capable of making its own launch decisions according to plan. Hainan Sounding Rocket Launch Site is capable of meeting these requirements.

At present, Hainan Sounding Rocket Launch Site can launch sounding rockets to altitudes of about 120 kilometers according to its own decisions and can fully complete telemetry data transmission, rocket flight path measurement, data collection, storage, and processing, reserve support in launch activities, and other tasks during rocket flight.

Hainan Sounding Rocket Launch Site will also be gradually outfitted with several pieces of scientific observation equipment for conducting comprehensive observations of the space environment. Excellent data have already been obtained on ionospheric anomalies using advanced ionospheric data probes installed at the launch site which are of major scientific importance. Using the favorable characteristics of Hainan Sounding Rocket Launch Site for domestic and international cooperative space science observations and research in equatorial regions is significant and attractive.

The CAS SSARC will cooperate with Germany's Max Planck Institute for Aeronomy in May 1991 to conduct observations and research of 1 to 3-meter plasma wave motion in the equatorial region ionosphere at Hainan Launch Site. They will also do research concerning the characteristics of biennial oscillations in the atmosphere of equatorial regions and how storms and lightning are propagated toward space near equatorial regions and their effects on the middle atmosphere. These are important topics for scientific research as well as research topics necessary for space technology development. If manned spacecraft are to be launched in near- equatorial regions, we must have a clear understanding of the atmospheric environment in the air above the launch region and recovery region. This is the safety corridor for manned spaceflight. Upper atmosphere rocket sounding research below 120 kilometers was required for very space shuttle test in the United States during the 1980's.

III. Development Ideas

Hainan Sounding Rocket Launch Site will gradually organize various types of small sounding rocket and certain technical system rocket flight tests and will come to play a greater role in space observation, research, and other areas. In addition, the CAS SSARC also envisages:

Developing a high-performance, low-cost 200 kilometer space environment rocket sounding system to create the conditions for longer term scientific research and applications and international cooperation;

Developing a high-performance, low-cost 300 kilometer microgravity rocket experiment system that can also be used for space biology and other comprehensive applied research.

Stochastic Hybrid Adaptive Control Scheme for Missile Control System

91FE0606 Beijing YUHANG XUEBAO [JOURNAL OF CHINESE SOCIETY AND ASTRONAUTICS] in Chinese No 2, 30 Apr 91 pp 21-28

[Article by Li Yanjun [2621 6056 0193] and Chen Xinhai [7115 0207 3189] of the Northwest Polytechnical University College of Astronautics: "Research on a Stochastic Hybrid Adaptive Scheme for a Missile Control System"; manuscript received 18 Oct 89]

[Text] Abstract: This article proposes a new stochastic system control scheme for use in tactical missile control systems—minimum variance hybrid self-tuning control. In this program, a control target with stochastic disturbance noise maintains a consecutive time state while control parameter estimation and readjustment are discrete, so the control law is a mixture of consecutive and discrete variates and the whole system is a hybrid stochastic system. Because this type of system combines the advantages of consecutive and discrete systems, it is a control system with very good prospects. This article introduces the basic principles of this type of control scheme and carries out a numerical simulation using a ground-to-air missile autopilot as an example. The results of the simulation show that the tracking performance of this type of hybrid adaptive scheme is superior to similar fully-discrete adaptive schemes. When system damping is relatively small, this superiority is especially prominent during the high altitude stage of missile flight.

Key terms: stochastic system, hybrid adaptive control, minimum variance, parameter estimation.

I. Introduction

Many Chinese and foreign scholars have been studying applications of adaptive control theory in aerospace engineering for years.

Because spacecraft operate in extremely complex and variable environmental conditions, it is very hard to pre-determine the laws of variation of these environmental conditions in normal situations. To ensure that control systems function well under all types of environmental conditions, adaptive control is an effective control method that deserves in-depth and extensive research.

Several articles concerning exploratory research on applications of adaptive control theory in aerospace engineering have been published in China and foreign countries. However, most of these articles describe fully-discrete systems and the few remaining ones concern fully-consecutive systems. To date, no one has discussed stochastic hybrid adaptive control systems.

Because most of the spacecraft which serve as control targets are themselves consecutive while fully-discrete methods are based on using real consecutive targets and discrete systems, their design cannot be closely coupled with real consecutive targets. Although consecutive time algorithms can be coupled with real targets, they are inconvenient for numerical operations and thus are not helpful in suppressing non-linearity and other dangerous effects. One control scheme for use in spacecraft control systems that has very good prospects is hybrid adaptive control.

This article proposes a consecutive time stochastic target minimum variance hybrid adaptive controller design method encountered during tactical missile engineering practice. When using this method to design adaptive control laws, no artificial consecutive time target discretization is required because it always maintains a consecutive time state, but control parameter estimation and readjustment are discrete and the whole system is a hybrid adaptive control system. Because this type of system combines the advantages of consecutive systems and discrete systems, it is a type of control system with very good prospects. This article carries out a numerical simulation using a ground-to-air missile autopilot as an example and the results of the simulation show that the tracking performance of this type of system is superior to similar full-discrete systems. When system damping is relatively small, this superiority is especially prominent during the high altitude stage.

II. Basic Principles of Stochastic Hybrid Adaptive Control

A single-input single-output consecutive time target is assumed

$$A'(s)y(t)=B'(s)u(t)+C'(s)\xi(t) \quad (2\text{-}1a)$$
$$A'(s)=s^{n}+a'_1s^{n-1}+\cdots+a'_n \quad (2\text{-}1b)$$
$$B'(s)=b'_0s^{m}+b'_1s^{m-1}+\cdots+b'_m \quad (2\text{-}1c)$$
$$C'(s)=s^{n}+c'_1s^{n-1}+\cdots+c'_n \quad (2\text{-}1d)$$

In the formulas, s = d/dt is the differential operator and $\xi(t)$ is high- frequency stochastic disturbance. B'(s) and C'(s) are Hurwitz polynomials, A'(s) and B'(s) are complements, and $n^* = n-m \geq 2$.

It is assumed that $q^{-1} = 1/1+\tau s$ where $\tau>0$ is the design constant. Thus, equation (2-1a) can be expressed by an equivalent equation

$$A(q^{-1})y(t)=q^{-n^*}B(q^{-1})u(t)+C(q^{-1})\xi(t) \quad (2\text{-}2a)$$
$$A(q^{-1})=1+a_1q^{-1}+\cdots+a_nq^{-n} \quad (2\text{-}2b)$$
$$B(q^{-1})=b_0+b_1q^{-1}+\cdots+b_mq^{-m} \quad (2\text{-}2c)$$
$$C(q^{-1})=1+c_1q^{-1}+\cdots+c_nq^{-n} \quad (2\text{-}2d)$$

Equation (2-2) has a similar form to the discrete time system but is entirely different in quality. In the discrete time system, q^{-1} represents the time delay, but since equation (2-2) is the consecutive time system, q^{-1} represents a single-stage filter. Because equation (2-2) is similar in form to the discrete system, formula derivation can be carried out using existing methods for processing discrete systems as a reference. Because there are qualitative differences between the two, however, the results of the discrete system derivation cannot be used directly here. Special attention should be given to these qualitative differences when actually carrying out formula derivation.

Our objective was to design a minimum variance hybrid self-tuning control system in a situation in which the target has stochastic disturbance to reduce the effects of the stochastic disturbance on system output to a minimum, which also means trying to have the system output y(t) track the parameter input signal r(t) as closely as possible. We also wanted to limit the control u(t) and prevent the required control signal from being too large.

To achieve this objective, we selected the index function

$$J=E\{[\bar{C}(q^{-1})y(t)-K\bar{C}(q^{-1})r(t)]^2+\lambda[q^{-n^*}u(t)]^2\} \quad (2\text{-}3)$$

In the formula, $\bar{C}(q^{-1})$ is a designer-selected polynomial

$$\bar{C}(q^{-1})=1+\bar{C}_1q^{-1}+\cdots+\bar{C}_nq^{-n} \quad (2\text{-}4)$$

Moreover, the nth differential polynomial $\bar{C}(s)$ obtained by multiplying $\bar{C}(q^{-1})$ by q^n is a Hurwitz polynomial.

First, the index function (2-3) is used to derive the optimum control law.

The design filter is q^{-1} and it is assumed that the high-frequency stochastic disturbance $\xi(t)$ is basically filtered out by a filter with more than one stage. Thus, $C(q^{-1})$ in equation (2-2) can be approximated as $C(q^{-1}) = 1$ when designing the controller. Based on actual recorded curves from tactical missile tests and actual working conditions of missile control systems, and in consideration of program feasibility, we feel that this assumption is reasonable. Thus, we can assume that the

polynomials $F(q^{-1})$ and $G(q^{-1})$ satisfy the relational expression:

$$\bar{C}(q^{-1}) = A(q^{-1})F(q^{-1}) + q^{-n^*}G(q^{-1}) \quad (2\text{-}6)$$

In the formula

$$F(q^{-1}) = 1 + f_1 q^{-1} + \cdots + f_{n^*-1}q^{-(n^*-1)} \quad (2\text{-}6)$$

$$G(q^{-1}) = g_0 + g_1 q^{-1} + \cdots + g_{n-1}q^{-(n-1)} \quad (2\text{-}7)$$

multiplying both sides of the equal sign (2-5) by y(t), we get

$$\bar{C}(q^{-1})y(t) = A(q^{-1})F(q^{-1})y(t) + q^{-n^*}G(q^{-1})y(t) \quad (2\text{-}8)$$

We can use formula (2-2a) to express the relational expression (2-8) as

$$\bar{C}(q^{-1})y(t) = q^{-n^*}B(q^{-1})F(q^{-1})u(t) + q^{-n^*}G(q^{-1})y(t) + F(q^{-1})C(q^{-1})\xi(t) \quad (2\text{-}9)$$

thus

$$J = E\{[q^{-n^*}B(q^{-1})F(q^{-1})u(t) + q^{-n^*}G(q^{-1})y(t) + F(q^{-1})C(q^{-1})\xi(t) - K\bar{C}(q^{-1})r(t)]^2 + \lambda[q^{-n^*}u(t)]^2\} \quad (2\text{-}10)$$

Based on the previous assumption concerning $\xi(t)$ and in consideration of the filtering action of filter q^{-1}, then $q^{-1}y(t)$, $q^{-2}y(t)$, ..., $q^{-(n+n^*-1)}y(t)$, $q^{-1}u(t)$, $q^{-2}u(t)$, ..., $q^{(n+n^*-1)}u(t)$ are unrelated to $\xi(t)$, so we can derive

$$J = E(\xi^2(t)) + E\{[q^{-n^*}B(q^{-1})F(q^{-1})u(t) + q^{-n^*}G(q^{-1})y(t) - K\bar{C}(q^{-1})r(t)]^2 + \lambda[q^{-n^*}u(t)]^2\} \quad (2\text{-}11)$$

Deriving the partial derivative of J in relation to $q^{-n^*}u(t)$ and setting it at 0, we can derive

$$\frac{\partial J}{\partial[q^{-n^*}u(t)]} = 2E\{q^{-n^*}B(q^{-1})F(q^{-1})u(t) + q^{-n^*}G(q^{-1})y(t) - K\bar{C}(q^{-1})r(t)]b_0 + \lambda q^{-n^*}u(t)\} = 0 \quad (2\text{-}12)$$

If we select u(t) to make

$$[q^{-n^*}B(q^{-1})F(q^{-1})u(t) + q^{-n^*}G(q^{-1})y(t) - K\bar{C}(q^{-1})r(t)]\,b_0 + \lambda q^{-n^*}u(t) = 0 \quad (2\text{-}13)$$

then $\delta J/\delta[q^{-n^*}u(t)]$ must be 0 and J is at a minimum. Thus we can derive the optimum control

$$u(t) = \frac{K\bar{C}(q^{-1})q^{n^*}r(t) - G(q^{-1})y(t)}{B(q^{-1})F(q^{-1}) + \lambda_1} \quad (2\text{-}14)$$

In the formula, $\lambda_1 = \lambda/b_0$ is the designer-selected normal constant.

To achieve the optimum control u(t) expressed by relational expression (2-14), we must estimate the unknown parameters in (2-14).

A. Indirect parameter estimation

Assuming

$$\theta^T = [a_1, a_1, \cdots, a_n, b_0, b_1, \cdots, b_m] \quad (2\text{-}15)$$

$$\zeta^T(t) = [-q^{-1}y(t), \cdots, -q^{-n}y(t), q^{-n^*}u(t), \cdots, q^{-(n^*+m)}u(t)] \quad (2\text{-}16)$$

then formula (2-2a) can be expressed as

$$y(t) = \theta^T\zeta(t) + \xi(t) \quad (2\text{-}17)$$

In the formula, y(t) and $\zeta(t)$ are physically attainable and directly measurable variables.

Carrying out discrete time sampling of y(t) and $\zeta(t)$ and assuming the time sequence to be unordered set: $t_k^{\infty 0}$ we can derive the discrete form equation corresponding to equation (2-17)

$$y(k) = \theta^T\zeta(k) + \xi(k) \quad (2\text{-}18)$$

In the formula, k represents the sampling instant t_k.

Based on equation (2-18) and using the derived sample values y(k) and $\zeta(k)$, we can select various identification methods to derive the estimated value $\theta(k)$ for the target parameter at instant t_k, so we can use equation (2-5) to determine estimated values for the unknown parameters in the control law (2-14). Because none of the variables in the vector $\zeta(k)$ are related to $\xi(k)$, θ can be consistently estimated using the identification algorithm provided in Section C of this article[5].

B. Direct parameter estimation

Multiplying both sides of the equal sign in formula (2-5) by y(t) and using formula (2-2a), we can derive

$$\bar{C}(q^{-1})y(t) = q^{-n^*}B(q^{-1})F(q^{-1})u(t) + q^{-n^*}G(q^{-1})y(t) + \xi(t) \quad (2\text{-}19)$$

Setting $B(q^{-1})F(q^{-1}) = \beta_0 + \beta_1 q^{-1} + \cdots + \beta_{n+n^*-1}q^{-(n+n^*-1)}$ (2-20)

and $\theta^T = [\beta_0, \beta_1, \cdots, \beta_{n+n^*-1}, g_0, g_1, \cdots, g_{n-1}]$ (2-21)

$$\zeta^T(t) = [q^{-n^*}u(t), \cdots, q^{-(n+n^*-1)}u(t), q^{-n^*}y(t), \cdots, q^{-(n+n^*-1)}y(t)] \quad (2\text{-}22)$$

$$y'(t) = \bar{C}(q^{-1})y(t) = y(t) + \bar{C}_1 q^{-1}y(t) + \cdots + \bar{C}_n q^{-n}y(t) \quad (2\text{-}23)$$

equation (2-19) can be expressed as

$$y'(t) = \theta^T\zeta(t) + \xi(t) \quad (2\text{-}24)$$

In the formula, y'(t) and $\zeta(t)$ are physically attainable variables. In doing discrete time sampling of y'(t) and $\zeta(t)$, we can use the sample information obtained from formula (2-24) for discrete estimation of control parameters.

After obtaining the estimated control parameter vector $\theta(k)$, physically attainable hybrid optimum control can be derived

$$u(t) = \frac{1}{\beta_0(k) + \lambda_1}\left[K\sum_{i=0}^{n}\bar{c}_i q^{-(i-n^*)}r(t) - \sum_{i=0}^{v-1}g_i(k)q^{-i}y(t) - \sum_{i=1}^{m+n^*-1}\beta_i(k)q^{-i}u(t)\right] \quad (2\text{-}25)$$

In the formula $\bar{c}_0 = 1$ and the $r(t)n^*$ exponent must be differentiable. Rational selection of parameter input signal r(t) is entirely capable of achieving this point.

Stability analysis of this type of system is related to the form of stochastic disturbance in the target and concerns selection of λ_1 and an actual identification algorithm. When the target stochastic disturbance sequence after filtering and sampling is a martingale differential series, a method similar to that in reference [4] can be adopted

to use a martingale convergence theorem and dimensional invariance principles to complete closed- loop system stability confirmation. When the target disturbance is bounded stochastic disturbance of another form, if the target input and output signals are bounded, it is easy to obtain closed-loop system stability confirmation. Those interested in a discussion of this question can refer to article [5]. We will not discuss it in further detail here due to space limitations.

It should be noted that, when carrying out control system stability analysis, the target equation must use formula (2-1) and not formula (2-2) because only formula (2-1) is a true target model whereas formula (2-2) is only an equivalent form equation for use in designing hybrid adaptive control laws.

III. Ground-to-Air Missile Hybrid Self-Tuning Control System Design and Numerical Simulation Results

Figure 1 is a simplified block diagram of a certain type of ground-to-air missile autopilot pitch channel.

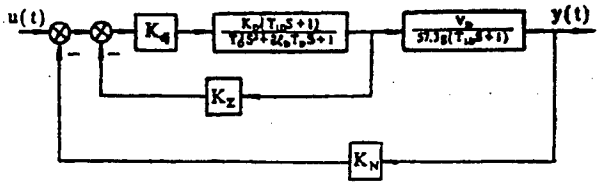

Figure 1. Simplified Block Diagram of Ground-to-Air Missile Autopilot Pitch Channel

The block diagram in Figure 1 can be used to derive the transfer function of a ground-to-air missile autopilot pitch channel

$$\frac{y(s)}{u(s)}=W(s)=A/(s^2+Bs+C) \qquad (3\text{-}1)$$

In the formula

$$A=K_1/T_1^2,\quad B=2\zeta_1/T_1,\quad C=1/T_1^2,$$

$$K_1=K_D^*V_D/(57.3g+K_D^*V_DK_N),\quad T_1=T_D\Big/\sqrt{1+\frac{K_D^*V_DK_N}{57.3g}},$$

$$\zeta_1=\zeta_D^*\Big/\sqrt{1+\frac{K_D^*V_DK_N}{57.3g}},\quad K_D^*=T_D/\sqrt{1+K_{d1}K_DK_z},$$

$$T_D^*=T_D/\sqrt{1+K_{d1}K_DK_z},\quad \zeta_D^*=\left(\zeta_D+\frac{K_{d1}K_DK_zT_{1D}}{2T_D}\right)\Big/\sqrt{1+K_{d1}K_DK_z}$$

Thus, the consecutive time target equation can be expressed as

$$(s^2+Bs+C)y(t)=Au(t)+(s^2+ds+f)\xi(t) \qquad (3\text{-}2)$$

In the formula, $\xi(t)$ is the high-frequency bounded stochastic disturbance.

Assuming that $\bar{C}(q^{-1})$, K=1, and the reference model

$$(s^2+28s+400)r(t)=400s(t) \qquad (3\text{-}3)$$

In the formula, s(t) is the square wave command signal and r(t) is the reference model output.

Using direct parameter estimation, assuming

$$\theta^T=[\theta_1,\theta_2,\theta_3,\theta_4] \qquad (3\text{-}4)$$

$$\zeta^T(t)=[q^{-1}u(t),\ q^{-2}u(t),\ q^{-1}y(t),\ q^{-2}y(t)] \qquad (3\text{-}5)$$

The chosen identification algorithm is

$$\theta(k)=\theta(T_i)+\theta_s(k)(k-T_i) \qquad (3\text{-}6a)$$

$$\theta_s(k+1)=\theta_s(k)+K(k+1)\left[\frac{y(k+1)-\theta^T(T_i)\zeta(k+1)}{k-T_i}\ \theta^T(k)\zeta(k+1)\right] \qquad (3\text{-}6b)$$

$$K(k+1)=P(k)\zeta(k+1)[1+\zeta^T(k+1)P(k)\zeta(k+1)]^{-1} \qquad (3\text{-}6c)$$

$$P(k)=P(k-1)-K(k)\zeta^TP(k-1) \qquad (3\text{-}6d)$$

See reference [6] for the principles and a detailed explanation of this type of identification algorithm.

The system hybrid optimum control form is

$$u(t)=\frac{1}{\theta_1(k)}[\,q^2r(t)-\theta_2(k)q^{-1}u(t)-$$

$$\theta_3(k)y(t)-\theta_4(k)q^{-1}y(t)\,] \qquad (3\text{-}7)$$

When doing parameter estimation, we assumed that q^{-1} = 1/(1+0.05s), the sampling period $T_s = t_k - t_{k-1}$ = 0.02 seconds, $\theta^T(0)$ = [2.119, 1.157, 0.353, 0.03], $\zeta^T(0)$ = [0, 0, 0, 0], the entire trajectory was divided into five time segments, T_1 = 6 seconds, T_2 = 14 seconds, T_3 = 22 seconds, T_4 = 30 seconds, T_5 = 38 seconds, and implementation of control started 6 seconds after launch. Figures 2, 3, and 4 show the actual simulation results. The added stochastic disturbance in Figures 2 and 3 is a white noise sequence with a mean of 0 and variance of 0.1 and 0.5, respectively. High-frequency colored noise stochastic disturbance was added in Figure 4. Figures 5 and 6 plot the addition of white noise and colored noise, respectively. Figures 7 and 8 show the system output curve obtained using the fully-discrete method under identical conditions. Comparison of Figures 2 and 3 with Figures 7 and 8 shows that the tracking performance of the hybrid self-tuning control scheme proposed in this article is superior to similar fully-discrete schemes and that the superiority of hybrid self-tuning control is especially prominent during the high altitude stage of flight.

IV. Conclusion

This article provides a rather detailed description of a stochastic system minimum variance hybrid self-tuning controller design scheme and the results of a ground-to-air missile hybrid self-tuning autopilot simulation. The results of the simulation show that this hybrid

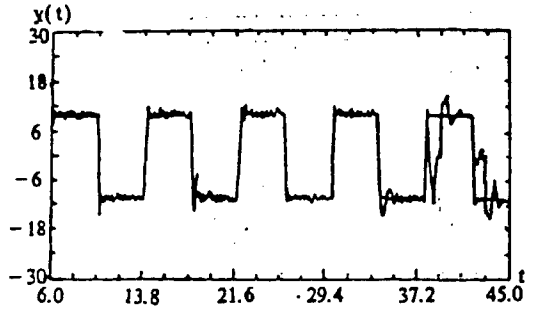

Figure 2. Output Curve of Hybrid Self-Tuning Control System When White Noise Stochastic Disturbance With a Mean of 0 and Variance of 0.1 Is Added (Square Wave in the Figure Is the Command Signal

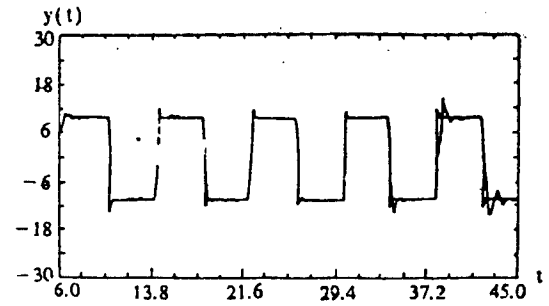

Figure 3. Output Curve of Hybrid Self-Tuning Control System When White Noise Stochastic Disturbance With a Mean of 0 and Variance of 0.5 Is Added (Square Wave in the Figure Is the Command Signal

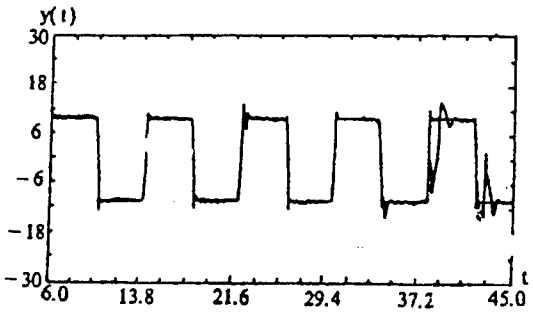

Figure 4. Output Curve of Hybrid Self-Tuning Control System When Colored Noise Stochastic Disturbance Is Added (Square Wave in the Figure Is the Command Signal)

self-tuning control scheme is superior to similar fully-discrete programs. Although this scheme requires practical testing, the results of initial research indicate that hybrid adaptive control has many advantages and is an effective control method that deserves broader and more extensive research.

The assumptions in this article concerning the control scheme and stochastic disturbance noise in the target

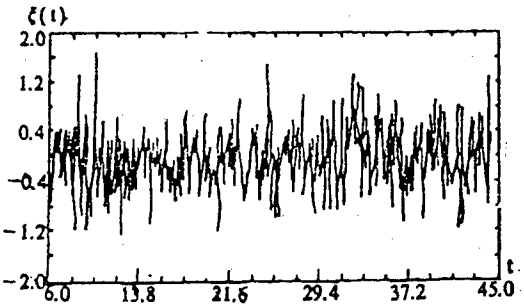

Figure 5. Plot of Stochastic Disturbance During Simulation When White Noise With a Mean of 0 and Variance of 0.5 Is Added

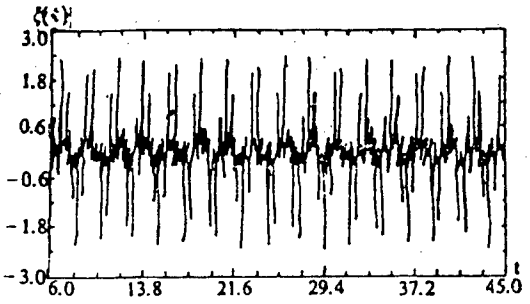

Figure 6. Plot of Simulation When Colored Noise Stochastic Disturbance Is Added

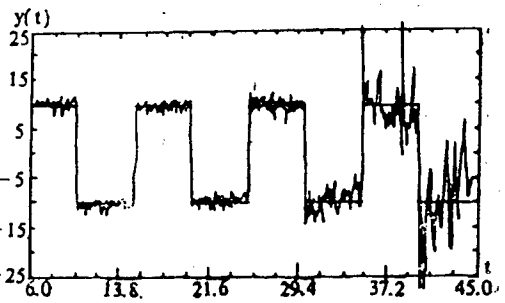

Figure 7. Output Curve of Fully-Discrete Self-Tuning Control System When White Noise Stochastic Disturbance With a Mean of 0 and Variance of 0.1 Is Added (Square Wave Is the Command Signal)

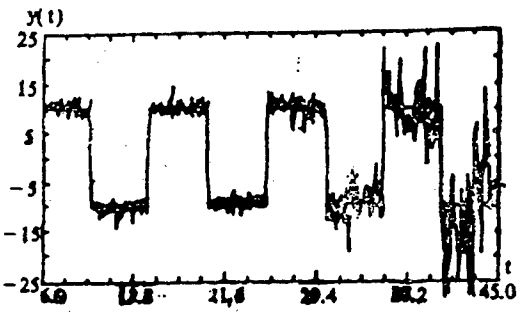

Figure 8. Output Curve of Fully-Discrete Self-Tuning Control System When White Noise Stochastic Disturbance With a Mean of 0 and Variance of 0.5 Is Added (Square Wave Is the Command Signal)

were based on a simplified method suggested by engineering practice with tactical missiles. For tactical missiles, especially ground-to-air missiles, the question of tracking command signals under high-altitude small damping conditions is the primary objective whereas the effects of stochastic disturbance that exist in the control system itself are not the primary question. Because all the variables adopted in parameter identification and control signal composition in the scheme in this article were basically filtered, this scheme is extremely beneficial in suppression of the effects of noise in the control system, so it can satisfy actual engineering requirements. As for noise generated by the guidance portion of the missile, we propose that other methods be adopted in the design for the steering head to eliminate it.

Of course, we can consideration even more normal noise models and carry out direct identification of the $c(q^{-1})$ coefficient like a discrete system, but since $\xi(t)$ cannot be measured, we can only carry out identification by substituting the corresponding residual error for $\xi(t)$. In a discrete system, because q^{-1} expresses the time delay, identification of the $C(q^{-1})$ parameter is feasible. In a hybrid control system, however, q^{-1} is a filter. It is hard for the post-filtering residual error in a tactical missile control system to satisfy sustained excitation conditions and correct identification of the $C(q^{-1})$ coefficient is difficult. The most important problem is still that there is no way to derive hybrid optimum control that is feasible in engineering terms. Of course, this is a topic that deserves further study in research on hybrid adaptive control theory, but this does not fall within the scope of this article.

References

[1] P. J. Gawthrop and D. Phil, Hybrid Self-Tuning Control, IEE Proceedings, Vol 127, 1980, pp 229-236.

[2] H. Elliot, R. Cristi, and M. Das, Global Stability of Adaptive Pole Placement Algorithms, IEEE Trans. on AC, Vol AC-30, 1985, pp 348-356.

[3] Takashi Suzuki, Haruo Kanamori, et al: Model Specifications for Hybrid Adaptive Control Systems, Proceedings of Conference on Measurement and Automatic Control, Vol 19, No 10, 1983.

[4] Li Yanjun [2621 6056 0193] and Chen Xinhai [7115 0207 3189], A Stochastic Hybrid Adaptive Controller, Xibei Gongye Daxue Xuebao (Journal of Northwest Polytechnical University), Vol 8, No 3, 1990.

[5] Li Yanjun, Hybrid Adaptive Control Theory and Its Use in Aerospace Engineering, Ph.D. Dissertation at Northwest Polytechnical University, May 1989.

[6] Chen Xinhai, Yan Xiaoming [7051 2556 2494], and Li Yanjun, A Rapid Time Varying Parameter Identification Method for Use in Aircraft Control Systems, Hangkong Xuebao (Journal of Aviation), Vol 11, No 9, September 1990.

Laser Small-Arms Simulator Developed

91P60226 Beijing ZHONGGUO KEXUE BAO [CHINESE SCIENCE NEWS] in Chinese 25 Jun 91 p 2

[Article by Bu Xiangqun [0592 0686 5028]: "Small-Arms Accurate Marksmanship-Practice Device Unveiled; Uses Laser Beam Instead of Bullets]

[Summary] A small-arms simulator, designed for improving marksmanship skills, has been developed by the CAS Institute of Semiconductors. The new system, which uses a laser-beam—instead of live ammunition—directed at fixed targets, has been put through trials in units of the Beijing Military Police and in civilian and military units of the Tong Xian district in Beijing Municipality. The new laser target-practice simulator, which provides a highly accurate means for practicing several types of firing, utilizes a Z8 single-board computer to control the laser-beam generation and results display and optoelectronic detectors to receive the laser signal at the target surface. Newly elaborated technologies include the lattice-structure detectors and light-spot memory compensation.

New Cell-Culture Reactor Developed

91P60223 Beijing ZHONGGUO KEXUE BAO [CHINESE SCIENCE NEWS] in Chinese 3 May 91 p 2

[Article by Zou Shuying [6760 3219 5391]

[Abstract] A new reactor for culturing hybridoma cells and producing monoclonal antibodies has been developed by the Dalian Institute of Chemical Physics and the Beijing Institute of Chemical Metallurgy. The reactor, based on the selective permeability of the hollow-fiber membrane introduced, effects substance exchange between two chambers to provide a suitable environment for cell propagation and favorable conditions for nutrient selection and metabolite separation in order to obtain high-density cell growth. With more than 200 grams of monoclonal antibody per milliliter cell culture and 9 x 10^7 cells per milliliter cell culture, the reactor can produce 1.5 grams of monoclonal antibody per month. To date, two different standards of hollow-fiber culture tubes have been developed to be used for the reactor.

Identification of Darna trima [more] Granulosis Virus [DTGV] and Its Characterization of Nuclear Acid and Protein

40091014A Chengdu SICHUAN DAXUE XUEBAO [JOURNAL OF SICHUAN UNIVERSITY—NATURAL SCIENCE EDITION] in Chinese Vol 28 No 2, May 91 pp 231-237

[English abstract of article by Yang Zhirong [2799 1807 2837], Liu Shigui [0491 0013 6311], et al., of the Institute of Biotechnology]

[Text] The virus, which had been isolated from Gong County of Sichuan Province in 1985, was identified as Darna trima [more]. According to the results of its infection test, pathologic study, ultrastructure observation of the inclutions and virions, analysis of nucleic acid type, and of DNA restriction endonuclease analysis, we know that the virus is a double-stranded DNA molecule with molecule weight of 64.11 x 10^6d, namely 93.87 kb. The result of its DNA melting test shows that its Tm Value is 67.3°C, namely the [G+C] content is 32.7 percent. The content of Asp and Glu in the inclution protein is 23 percent, but that of His, Cys and Met are very low. Because of its great ability to infect the larva of Darna trima, the virus has great potential applicability in biological control.

Study on Parameter Identification of Fuzzy Control Model on Human Control Behavior

40091014B Beijing YUHANG XUEBAO in Chinese No 2, Apr 91 pp 78-85

[English abstract of article by Huang Junlin [7806 0193 2651] of Institute 303 of the Ministry of Aerospace and Long Shengzhao [7893 0581 3564] of the Institute of Space Medicine and Medical Engineering]

[Text] In study of a human control process, it is a very complex, difficult step, and an importance in this field, to determine the parameters of human fuzzy control model. Resolving of the problem will be significant to the study, analysis and design of man-machine control system. This paper presented a parameter identification method based on the structure of human fuzzy control model known, and tried to identify parameters of the model. Results obtained so far show that the said method is very simple, efficient and useful. The method not only provides basic data for research of the model, but also proposes a new approach to study of parameter identification.

More on Nation's First Major High-Speed Composite Computer LAN

91FE0648B Beijing ZHONGGUO KEXUE BAO [CHINA SCIENCE NEWS] in Chinese 24 May 91 p 3

[Article by Chang Jiachen [1603 3946 6591]: "China Completes Composite Local Area Computer Network"; cf. earlier report in JPRS-CST-91-013, 20 Jun 91 pp 5-6]

[Text] China's first large-scale high-speed composite local area computer network [LAN] has now been completed by the China Research Institute of Atomic Energy Sciences [RIAES]. The famous nuclear physicist Wang Ganchang [3769 3227 2490] cut the ribbon to commemorate the project and watched a demonstration of network system functions.

The RIAES computer network was designed and installed in cooperation with Hong Kong's Geotech Company and overcame many technical difficulties. It is composed of an optical cable ring network and six Ethernets. It uses TCP/IP [transmission control protocol/internet protocol] protocol to enable interconnection of different types of computers, and it has high-speed communications functions. It can not only satisfy RIAES requirements for fast neutron breeder reactor and nuclear power plant design, nuclear power safety analysis, nuclear physics research, accelerator design, and other high-tech development project and service management, but also can provide experience for extension to large research units in China that are developing computer network applications.

Domestic Software Entering International Market

91FE0648A Beijing JINGJI RIBAO in Chinese 22 May 91 p 2

[Article by Liu Keli [0491 0344 7787] and Wang Yuling [3769 3768 3781]: "Chinese Software To Enter International Market"]

[Text] If the 20th Century can be called the golden age of computer hardware, then the 21st Century will be the golden years for computer software.

With the ever-growing improvements in the performance, price, reliability, and degree of integration of large-scale integrated circuits, the human labor costs for the world's computer hardware will drop to 2 percent of overall computer hardware systems by the end of this century while marketing, repair, and other services and software labor costs will gradually rise. This is particularly true for software human labor costs, which will rise to 75 percent of the overall cost of computer systems.

In the world today, the volume of sales in software markets has grown at a yearly rate of 30 percent. Behind this figure is an obvious disparity in the growth of software labor services in the developed nations and developing nations. In the United States, the world's number one computer power, if there are 10 million pieces of software that await people for development, that would mean a shortage of 500,000 skilled software laborers! Facing the shortage of skilled personnel in world software markets, the developed nations began in the late 1980's to form a tidal flow of software labor service exports. In India, for example, the volume of software exports during 2 consecutive years, 1989 and 1990, exceeded $10 billion.

What can China do to deal with this world situation?

China now has 100,000 specialized computer personnel and over half of them have been or are now involved in software development. China's volume of software exports in 1989 was $7 million and grew to $10 million in 1990. Although the base figures are still much smaller than other software exporting countries, computer software has already become a powerful force that cannot be ignored in China's high-tech industry exports.

At present, China's software exports overall fall into these models:

The liveliest software export model is software labor service exports, in which China sends out software labor services while simultaneously bringing technology from the developed nations back into China, training software technical forces in China, and accumulating forces for China's future software development. For the past 5 years, the Beijing Municipality Software Services Association has actively promoted and guided software export work and they have made substantive explorations on conducting software labor service exports with the China-Japan Computer Technology Exchange Association. They have recruited recent graduates in computer software specializations and, after strengthening training in Japanese and passing tests given by the Japanese side, they have been reassigned to engage in software work for 3 years in over 40 medium-sized enterprises under the jurisdiction of the China- Japan Computer Technology Exchange Association. During these 3 years, they will not only earn foreign exchange for the state but can also attain the goal of training this group of top-quality personnel as system analysts (the highest skill level in the computer software profession). Now, the first group of 32 young people have begun working in Japan since the end of March 1991 and the second group of 80 personnel will begin Japanese language training in mid-April 1991. Qinghua University has consistently signed data entry contracts with the Pacific Company in the United States over the past 10 years. Particularly noteworthy have been the past 2 years, when they have earned about $900,000 in foreign exchange income for the state each year. Although this model for software exports is only the initial phase of software exporting, analysis of the level of computer popularization in China indicates that there will be a trend toward continued growth in the future.

The model of assuming contractual responsibility for software projects has just begun to grow in China's software industry. It involves processing various types of software according to the requirements of customers in

foreign countries and delivering them on schedule. This type of arrangement is also a higher-level phase of software exporting that involves no market risks and provides obvious economic benefits. Xinxin Software Company Ltd. in Shekou, Shenzhen, China has just 150 people but it earned $1 million in foreign exchange for the state in 1990. They have established computer networks with the United States, Singapore, Hong Kong, and other countries and regions, reduced the distance from international markets and also reduced product delivery schedules, and they formed a product mix in which multi-media software is the leading product.

In addition, product marketing, cooperative development, establishment of Chinese-foreign joint investment software companies, and other arrangements are future directions for software exports. In 1990, China established cooperative relationships or opened joint investment plants with the IBM Corporation, DEC Corporation, and Hewlett-Packard Corporation, three of the world's big computer companies, and one of the objectives was to aid China's software exports.

Several unfavorable factors currently exist in the development of China's software exports, such as a trend toward revaluation of China's abundant software labor resources, the negative outflow of skilled personnel which accompanies exports of software labor services, lack of clarity concerning the responsible administrative units, and so on, but we are still keeping pace with rapidly developing world software markets and there can be no doubt concerning their enormous development potential.

Nation's First Copyrighted Chinese Microcomputer System Passes Appraisal

91P60214C Beijing ZHONGGUO DIANZI BAO [CHINA ELECTRONICS NEWS] in Chinese 16 Jun 91 p 1

[Article by Mao Xifang [0379 6932 5364]: "Nation's Only Copyrighted Chinese-Language System—EC386 Microcomputer System—Passes Appraisal"]

[Summary] The EC386 microcomputer system, independently developed by the East China Computing Technology Institute in Shanghai, passed appraisal on 16 May in Shanghai. The EC386, the nation's only copyrighted Chinese-language microcomputer system, is now being put into mass production, with an annual output that can reach 50,000 units. The entire system includes the copyrighted high-performance Chinese-language software system, and Western software not requiring Chinese-character conversion can be run directly. The EC386 is compatible with IBM main-stream computers.

Nation's First Workstation Joint Venture Established

91P60214B Beijing JISUANJI SHIJIE [CHINA COMPUTERWORLD] in Chinese No 22, 5 Jun 91 p 1

[Article by Li Qingci [2621 3237 1964]: "China's First Joint Venture for Producing Computer Workstations Opens for Business in Shanghai"]

[Summary] Huapu [5478 2528] Information Technology Ltd., the nation's first Sino-foreign joint-venture firm to manufacture computer workstations, formally opened for business on 27 May in the Hongqiao Economic Development Zone in Shanghai. Among the dignitaries who attended the opening ceremonies were MMEI Vice Minister Zeng Peiyan and Shanghai Vice Mayor Liu Zhenyuan. The new firm, a joint venture between MMEI's East China [Hua Dong] Computing Institute and the U.S. company Hewlett Packard [Hui Pu], has an aggregate investment of US$9 million, with registered capital of US$4.5 million; it is the third joint-venture workstation partner that HP has taken worldwide. Huapu Information Technology Ltd. will engage in the development, manufacturing, and sales of HP's Apollo workstations and in the export of software.

Integrated Services LAN Developed

91P60214A Beijing JISUANJI SHIJIE [CHINA COMPUTERWORLD] in Chinese No 22, 5 Jun 91 p 13

[Article by Ding Quanlong [0002 3123 7893]: "Integrated Services Local Area Network Developed"]

[Summary] A voice/data packet-switching integrated services LAN developed by Xidian University passed the appraisal conducted the other day by MMEI in Xian. This LAN employs the token bus format, with an improved TCP [transmission control protocol] protocol and IEEE802.4 protocol. Bus transmission rate is 2.048 Mbps, transmission range is 1,500 meters, number of telephones connectable is 32, and number of data workstations is 32. The new LAN is designed to connect IBM PCs and common telephones and has fully distributed control (no central server); it is oriented toward industrial, office automation, and military applications.

Copyrighted DBMS Set Unveiled

91P60229 Beijing ZHONGGUO DIANZI BAO [CHINA ELECTRONICS NEWS] in Chinese 23 Jun 91 p 1

[Article by Lin Feng [2651 2800]: "New Breakthrough in Development of Domestically Made Database Management System"]

[Summary] An independently copyrighted complete set of database management systems (DBMSs) developed in a 10-year effort by engineers at Central China (Huazhong) University of Science & Technology was recently unveiled. The new domestically made DBMS set consists

of an SQL [structured query language] standard DBMS called HDB, a map data management system called MDB, a knowledge-base management system called KDB, and a graphics DBMS called GDB. These various systems separately passed technical appraisals held in Beijing 11-13 June by the State Education Commission, by various electronics research institutes under MMEI, and by the National Natural Science Foundation's (NSFC) Information Science Department.

HDB includes a complete Chinese-character interface, a word processor and editor, a dynamic index, and full define-search functions; with some further commercialization, this product can replace foreign-made DBMSs intended for mid-sized computers and minicomputers. MDB is a graphics/image/word/complex-object-oriented multimedia DBMS. KDB, developed in the NSFC-supported "distributed knowledge database" project, integrates artificial intelligence and database technologies, and provides a convenient environment for establishment of expert systems. GDB is a practical tool for managing graphics and conventional data; it is especially strong in resolving problems involved with dynamic increases in graphics memory, and is a strong tool and environment for CAD/CAM and computer information management systems.

New World-Class Achievements in X-Ray Laser Research Reported

91P60220A Beijing GUANGMING RIBAO in Chinese 24 Jun 91 p 1

[Article by Liu Jingzhi [0491 2417 2535]: "Major Advances Realized in Nation's X-Ray Laser Research"]

[Summary] It has been learned from authoritative sources that the nation's X-ray laser researchers have realized major new advances—in some respects taking a leading position worldwide. During the Seventh Five-Year Plan, Chinese scientists made several advances with their "Shen Guang" high-power laser facility in areas such as plasma diagnosis, target-arrangement technology, theoretical and mathematical simulation, and experimental research. In recent experiments with butt-jointed double targets, Chinese scientists achieved a gain-length product (GL value) of 15 [cf. JPRS-CST-91-013, 20 Jun 91 pp 9-10], the highest value obtained among researchers from similarly equipped laboratories worldwide. Employing their NOVA facility, which is over 100 times more powerful than the Chinese apparatus, U.S. scientists at Lawrence Livermore National Laboratory have obtained a GL value of 16. Moreover, the continuous time for thick-target X-ray lasing achieved by Chinese scientists is much longer than that realized by U.S. scientists; critical to this achievement is the use of reflectors as cavity resonators and improvements in beam quality.

Following upon the first domestic realization of 1089-angstrom xenon laser output—an achievement researchers from the China Academy of Engineering Physics reached via application of the photo-ionization Auger effect—the nation's scientists continued to study photo-ionization mechanisms, composite mechanisms, and collision mechanisms to achieve X-ray lasing. Employing a composite mechanism, researchers from the CAS Shanghai Institute of Optics and Fine Mechanics in experiments on Li-like Al laser gain have reached X-ray laser wavelengths shorter than 100 angstroms. Other internationally noteworthy achievements include the first reported development of a cylindrical-array-lens optical focusing system, which improves the uniformity of the intensity distribution of the laser focal lines, and the development of a grazing-incidence-grating spectroscope whose time resolution has reached the state-of-the-art.

World's First Laser-Heat-Treatment Seamless-Tube Oil Pump Production Line Constructed

91P620212C Beijing GUANGMING RIBAO in Chinese 8 Jun 91 p 1

[Article by Xu Jiuwu [1776 0046 2976]: "CAS Institute of Mechanics Teams Up with Industry To Construct First Laser Heat Treatment Production Line"]

[Summary] At a press conference held on 4 June, senior engineer Zhang Xiuqin from the CAS Institute of Mechanics and Tianjin Dagang Petroleum Drilling & Extraction Machinery Plant director Zhao Guowen announced that the nation's first production line for long seamless-steel-tube oil pumps fabricated via laser heat treatment has been formally completed. It is understood that this facility, jointly constructed by the two aforementioned organizations, is the first of its kind reported worldwide. The new production line is designed for one-step processing of the inner wall of various types of 8-m-long (or 15-m-long, with heat adjustment) large-aperture (56-mm-and-up) seamless-tube pumps, and permits ultrafine martensitic quenching for greatly increased abrasion resistance. Compared to conventionally processed tube, this new high-energy-laser-beam treatment increases efficiency by 30 percent, prolongs life by 100-200 percent, and greatly reduces cost. If all the nation's mechanical oil-extraction wells were to convert to this new pump when their old ones wear out, each year of increased life would save the state over 400 million yuan. The new production line also can be used for automotive, shipbuilding (processing of steamship cylinders), and military purposes.

New High-Speed Laser Measurement Systems Developed

91P60212B Beijing ZHONGGUO KEXUE BAO [CHINESE SCIENCE NEWS] 4 Jun 91 p 2

[Article by Zhang Jianping [1728 1696 1627]: "Anhui Institute of Optics & Fine Mechanics Develops Two New High-Speed Laser Measurement Systems"]

[Summary] A National Defense Science, Technology & Industry Commission Seventh 5-Year Plan key project assigned to the CAS Anhui Institute of Optics & Fine Mechanics (AIOFM) and involving the development of a "laser bidirectional reflection-distribution-function measurement system" and a laser autoreflection measurement system" recently passed CAS-level appraisal. The former system, a critical technique for studying laser scattering characteristics, creatively integrates laser technology, optomechatronics technology, and computer data processing & control technology; along with an AIOFM-developed software package for total computer control, this high-speed, high-accuracy system should be of value in defense modernization and in civilian high-tech areas. The latter system integrates infrared laser technology, optomechatronics technology, and computer processing & control technology; it can be used for measuring pulsed or CW laser characteristics. The experts at the appraisal agreed that these two new laser measurement systems—one of which is shown in the accompanying photograph—have reached the late-eighties international level.

The photo shows institute engineers describing the laser autoreflection measurement system's performance and operating conditions to the expert appraisal panel.

Coaxially Pumped Optical Fiber Dye Laser Studied

91P60212A Shanghai ZHONGGUO JIGUANG [CHINESE JOURNAL OF LASERS] in Chinese Vol 18 No 5, May 91 p 332

[Letter by Lu Xuebiao [7120 7185 2871], Chen Yangqin [7115 2254 7485], and Qiu Mingxin [6726 2494 2450] of the Shanghai Institute of Laser Technology, 200233: "Coaxially Pumped Optical Fiber Dye Laser"; project supported by NSFC, MS received 7 Aug 90]

[Summary] Based on our study of a Raman liquid-core optical fiber laser, we have carried out detailed research on a coaxially pumped liquid-core-fiber dye laser. We chose benzyl alcohol as the solvent for forming the liquid-core-fiber waveguide, since the index of refraction (n = 1.46) of benzyl alcohol is higher than that of quartz for the liquid-core-fiber cladding material; moreover, its fluorescent quantum yield is very low—most of the excited dye molecules are quenched by the solvent. Our final solvent—a transparent colorless benzyl alcohol solution—had an index of refraction of 1.539. In an experiment comparing a benzyl alcohol-rhodamine 6G solution in an ordinary dye laser to a solution of ethanol-rhodamine 6G of the same concentration, we observed a lower fluorescent efficiency, but could obtain [desirable] laser oscillation.

In the laboratory, our hollow optical fiber, drawn from quartz material, had an I.D. of 500μm, an O.D. of 1000μm, and a length of 12 cm. A capillary tube was employed to inject the 1 x 10^{-4}M [molar] benzyl alcohol-rhodamine 6G dye solution into the fiber. The pumping light was obtained from a Q-modulated pulsed YAG laser frequency-doubled by a KDP [potassium dihydrogen phosphate] crystal; wavelength was 532.1nm, pulse width was 10ns, and a maximum monopulse energy was 2mJ. The laser beam was focussed and coupled into the fiber via a lens with a 2-cm focal length.

In determining the relationship between pumping intensity and fiber output-end signal intensity, we noticed that the plotted curve has two slopes. When pumping intensity is low, fiber output intensity rises only very slowly with increasing pumping intensity; but when the intensity of the pumping light exceeds a threshold of 3.44 x 10^7 W/cm^2, output light intensity increases in rapid linear fashion, indicating initial laser oscillation. For a measured pumping light energy of 2mJ, the energy of the dye laser at the output reached 0.21mJ, with a beam divergence angle of 12°. Laser flare assumed a multimode form. Since there are no reflecting lenses for energy feedback at the two ends of the fiber, this coaxially pumped fiber dye laser is essentially a travelling-wave-amplifier laser.

Refractive Index Measurement of Nd:MgO:$LiNbO_3$ Crystal and Its Self-Frequency-Doubled Laser at Room Temperature

40100060A Shanghai ZHONGGUO JIGUANG [CHINESE JOURNAL OF LASERS] in Chinese Vol 18 No 5, May 91 pp 324-328

[English abstract of article by Xu Guanfeng, Gong Mali, Guo Yongjin, Chen Jiarong, Li Bin, Zhai Gang, and Han Kai of the Southwest Institute of Technical Physics, Chengdu; MS received 17 Sep 90]

[Text] Refractive index measurement of the Nd:MgO:$LiNbO_3$ crystal and its self-frequency-doubled laser at room temperature are reported for the first time. Net SHG [second harmonic generation] green output at 400 μJ/shot has been obtained with a small Xe lamp pump at 26°C. The threshold pump energy is smaller than 4.8 J. The laser operates over 25-45°C. No photorefractive damage was observed.

A Real-Time Method for Fourier Transform Holographic Information Storage

40100060B Shanghai ZHONGGUO JIGUANG [CHINESE JOURNAL OF LASERS] in Chinese Vol 18 No 5, May 91 pp 385-386

[English abstract of article by Cai Tiequan, Wang Hui of the Physics Department, Zhejiang Normal University, Jinhua, and Tian Zhiwei of the Physics Department, Hangzhou University, Hangzhou; MS received 28 Apr 89]

[Text] A method is put forward by which the Fourier transform hologram is recorded in real time. By using the incoherence-coherence property of LCLV (liquid crystal light valve) as an image-conversion device, documents and pictures can be stored directly with Fourier transform holography.

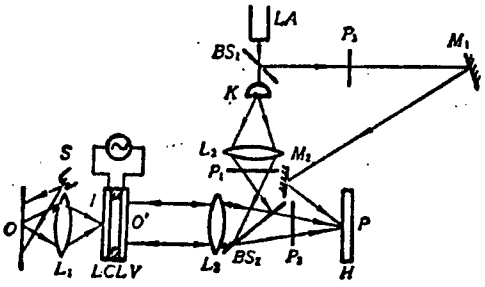

Figure 1. An Experimental Setup for Recording Real-Time Fourier Transform Hologram of Data

28 Kinds of Space-Qualified, Radiation-Hardened CMOS ICs Pass Appraisal

91P60215A Beijing ZHONGGUO DIANZI BAO [CHINA ELECTRONICS NEWS] in Chinese 7 Jun 91 p 5

[Article by Ding Yanshen [0002 3601 3947]: "CMOS Integrated Circuits for Long-Life Communications Satellite Equipment Pass Appraisal"]

[Text] Designed for use in long-service-life communications satellite equipment, 28 varieties of radiation-hardened, space-qualified silicon-aluminum-gate CMOS ICs developed by Beijing Municipal Semiconductor Device Plant 3 passed technical appraisal on 28 May. The new ICs' indicators for resistance to radiation doses and for reliability all comply with satellite contract specification requirements, and fill a domestic void. These products' [developers] completely relied on their own technical forces, and gradually worked out the production technology for realizing radiation hardening, including batch production of the ICs.

Interview With Huajing Electronics Group's General Manager

91P60224 Hong Kong LIAOWANG [OUTLOOK] OVERSEAS EDITION in Chinese No 26, 1 Jul 91 pp 17-18

[Article by Chen Lian [7115 5114] and Lu Yongfang [7120 3057 5364]: "Accelerate Development of Nation's Microelectronics Industry: Interview with Huajing Electronics Group's General Manager Su Guangping"]

[Summary] The Huajing Electronics Group (HEG), located in scenic Wuxi City [Jiangsu Province], is one of the leading integrated teaching/research/production/marketing enterprises in the nation, and its annual output of all types of ICs has represented one-third of the national IC output for each of the past 5 years (and 70 percent of the national output of ICs for TV sets). Recently, this writer interviewed HEG's General Manager, Su Guangping [5685 1639 1627], who commented on HEG's past, present, and future.

HEG grew out of a union between the locally administered Jiangnan Radio Equipment Plant state enterprise (built in 1960) and the Wuxi branch of the Ministry of Electronics Industry's Research Institute 24. This union, then called Wuxi Microelectronics Integrated Corporation (WMIC), was responsible for development of the nation's first VLSI—a 64-kilobit DRAM. In August 1989, with WMIC at its core, China HEG was formally born out of the merger of 70 firms.

Today, HEG—with an annual output of 50 million ICs, 100 million discrete devices, and 300 million chips—is the nation's largest microelectronics research and production base. Its basic goal is to further develop toward a market-guided, S&T-driven corporation that will remain competitive through new-product development, improvement in yields, cost reduction, and exploration of new market routes. As examples of HEG's new products, he mentioned various ICs used in color and black and white TV sets, in telephones, and in TV remote-control units, and high-, mid-, and low-power transistors. New product sales for 1990 constituted 34 percent of the group's gross sales for that year.

In order to improve the level of the domestic microelectronics industry, HEG and the state are jointly investing almost a billion yuan in the construction of an advanced MOS [metal oxide semiconductor] IC large- scale production line and research training line during the [current] Eighth 5-Year Plan. Work on this project is currently being stepped up, and formal operation is planned for 1993. Mr. Su concluded with an analysis of the gap that china must overcome to become truly competitive with the developed foreign nations, which are now putting 16-megabit DRAMs into production and carrying out research on 64-megabit DRAMs.

K_xC_{60} Superconductor Synthesized by Beijing University, CAS Institute of Physics

91P60232 Beijing RENMIN RIBAO in Chinese 17 Jul 91 p 3

[Unattributed article: "Further Advances in Research on New Superconducting Materials"]

[Summary] Following upon their successful synthesis of C_{60}—the newly discovered (1985) third allotropic form of carbon [now known as buckminsterfullerene]—in early June, scientists in the Chemistry and Physics Departments at Beijing University joined forces with colleagues in the CAS Institute of Physics and successfully synthesized the compound superconductor K_xC_{60} on 9 July. Testing of AC magnetic susceptibility at a key state laboratory indicates that samples of the new compound have a transition temperature of 17.9K.

It was only in April of this year that scientists at Bell Labs in the U.S. first succeeded in synthesizing an alkali-metal-doped compound of C_{60} that exhibited superconductivity—a discovery arousing worldwide interest. According to overseas reports, K-doped C_{60} has shown a transition temperature of 19.3K, while Rb-doped C_{60} has shown a transition temperature of 30K. Having heard of this report, the Beijing University researchers began their own research project on 28 May, and on 10 June succeeded in synthesizing C_{60} of relatively high purity. They and their CAS Institute of Physics colleagues quickly followed this up with synthesis of alkali-metal-doped C_{60} (K_xC_{60}) with a transition temperature only slightly below the leading international value. Moreover, these researchers are now studying Rb-doped C_{60} and its superconductive properties.

Feature on Specialist in Superconducting Electronics

91P60221A Beijing GUANGMING RIBAO in Chinese 19 Jun 91 p 2

[Article by Yang Kaimin [2799 7030 3046]: "Daring To Be First in Cutting-Edge Area: Wu Peiheng and His Achievements in Superconducting Electronics"]

[Summary] Wu Peiheng [0702 1014 0077], a scientist trained in the New China era, was 22 when he graduated from Nanjing University in 1961 with a major in physics. Staying on as a graduate assistant and then as an assistant professor, he specialized in research on superconducting electronics, and developed several superconducting electronic devices—such as a microwave receiver—that operated at liquid-helium temperature.

Made an associate professor in April 1980, he studied in Britain for almost two years, returning to China in December of 1981 to lead a research group. He and his group threw themselves into the international race that began with the announcement of high-temperature (liquid-N-temperature) superconductors. One of the important projects the group has worked on in the past few years is the development (announced in the latter half of 1987) of a liquid-N-temperature fundamental-wave mixer, a critical component for high-frequency signal reception in communications, radar, and radiotelescope systems. This development, the first of its kind reported worldwide, was followed by the group's development of a superconducting harmonic-wave mixer and a self-local-oscillation mixer.

Wu Peiheng was made full professor in April 1985, and in 1989 he was appointed chairman of the newly created offshoot, the Information Physics Department, at Nanjing University. In addition to continuing his research pursuits, he is the graduate student adviser.

X-Band Superconducting Nb Cavity

40100062A Hefei DIWEN YU CHAODAO [CRYOGENICS AND SUPERCONDUCTIVITY] in Chinese Vol 19 No 2, May 91 pp 46-48

[English abstract of article by Wei Xinqi and Wang Cheng of the Hefei Research Institute of Cryogenics and Electronics; MS received 5 Feb 91]

[Text] The research results of a superconducting cavity made of pure Niobium materials from China are presented. The experimental system and the measuring method are described. At 4.2K, a Q_0 [unloaded quality factor] value of 1.01×10^7 is obtained in the TE_{011} mode cavity at a frequency of 9.9 GHz.

Measurements of Response of Superconducting Mixer at Liquid-Nitrogen Temperature

40100062B Hefei DIWEN YU CHAODAO [CRYOGENICS AND SUPERCONDUCTIVITY] in Chinese Vol 19 No 2, May 91 pp 49-52

[English abstract of article by Yang Shihong, Cai Anjiang, and Liu Xinhua of the Hefei Institute of Cryogenics and Electronics; MS received 5 Feb 91]

[Text] A "large bridge" junction made of bulk YBCO has been developed. At the temperature of liquid nitrogen, the response of a mixer is obtained by applying a local oscillating signal (f_L = 33.1 GHz) and a measuring signal (f_S = 33.35 GHz) in the waveguide cavity. The response curve of intermediate-frequency (IF) output power by applying dc-bias on the junction is measured, and the IF spectral response curve is recorded by spectrum analysis.

References

1. P. H. Wu, et al., Vol 25. 2, March 1989 IEEE.

2. John Clarke, "Principles and Applications of SQUIDs," PROCEEDINGS OF THE IEEE, Vol 77, No 8, August 1989.

3. S. Q. Xue, J. Zhang, et al., "High-T_c RF-SQUID Magnetometer and Its Applications," ICEC-13, April 24-27, 1990, Beijing, P. R. China.

Microwave Surface Resistance of Ceramic Superconductor $YBa_2Cu_3O_{7-x}$

40100062C Hefei DIWEN YU CHAODAO [CRYOGENICS AND SUPERCONDUCTIVITY] in Chinese Vol 19 No 2, May 91 pp 53-56

[English abstract of article by Liu Dong, Yang Tao, and Chen Xinhang of the Department of Physics, Northwest University; Li Jianping, Wang Jingrong, and Wu Xiaozu of the Northwest Research Institute of Nonferrous Metals; and Wang Jiasu, Wang Suyu, and Tang Qixue of the Department of Applied Physics, Southwest Jiaotong University; MS received 20 Oct 90]

[Text] Two YBCO cavity resonators that have different J_c [critical current density] have been carefully prepared, almost by the same technique. Both of them have Q [quality factor] about 10^5 at 10 GHz. The measured results suggest that samples which have high J_c show narrow transition width of R_s [surface resistance], and those which have low J_c show larger width. These facts mean that R_s as well as J_c is closely related to the properties of the grain boundaries of high-T_c superconductors.

Ultra-Short-Wave Radiotelephones Exported to USSR

91P60227B Beijing ZHONGGUO DIANZI BAO [CHINA ELECTRONICS NEWS] in Chinese 26 Jun 91 p 2

[Article by Ren Guangquan [0117 0342 3123] and Wang Guocai [3769 0948 2088]: "Domestic Communications Equipment Has Great Market Potential in Soviet Union, East Europe; A Discussion of Plant 716's Export of Communications Systems to the USSR"]

[Summary] In March of this year, 150MHz ultra-short-wave three-circuit duplex radiotelephones manufactured by Plant 716 were exported to the USSR, and Chinese engineers were dispatched to install and debug the equipment and to assist authorities in a Ukrainian city in setting up a regional wireless communications network. After this network became operational, the Soviet technical experts at the acceptance check appraised it as advanced, practical, and of good communications quality.

Since 1984, when this radiotelephone was first put into production by Plant 716, over 2,000 sets have been manufactured and put on the market. Product quality now meets mid-eighties international standards.

It has been learned that the USSR and several East European nations plan within the next 10 years to expend huge sums on purchase of communications equipment to modernize their information industries. The Chinese have experience in setting up inter-telephone-office communications based on stored-program-controlled exchanges interconnected with this type of small-capacity wireless communications system, which manifests no interference on any channel and has unusually clear voice reproduction; the Soviets and East Europeans, on the other hand, do not have strength in development of 150MHz civilian communications equipment. The arrangement has opened up a new marketing route for this product, the domestic market for which—concentrated in transportation, mining, petroleum exploration, forestry, and rural communications—has contracted in recent years.

Guilin Plant Has Record Sales of PCM480 DMW Equipment

91P60227A Beijing ZHONGGUO DIANZI BAO [CHINA ELECTRONICS NEWS] in Chinese 26 Jun 91 p 1

[Article by Zhou Deshao [0719 1795 4801]: "Li River Plant Converts New-Product Marketing Strategy into Coordinated Production-Marketing Growth"]

[Summary] The Guangxi [Province] Guilin Li River Radio Plant has lost no time in implementing a new marketing strategy: coordinated growth of production and sales, centered on its main product, the PCM480 [pulse code modulation 480-circuit] digital microwave (DMW) communications system, a 1980's-level product manufactured with production-line technology imported from Japan's NEC in 1988. In the first 5 months of this year, the plant fulfilled contract orders for 86 complete sets, amounting to 80 percent of the planned output for the entire year. This quantity of orders is equivalent to three times the amount for all of last year, and sales income has risen over 800 percent compared to the same period last year.

The Guilin plant's new strategy includes representation at national and international high-tech fairs, as well as sales of spare parts and provision of maintenance services. Government departments that have already placed orders for the PCM480 DMW system include Energy Resources, Transportation, Electric Power, P&T, and Water Resources. Some units that were preparing to apply for foreign exchange to import similar equipment from abroad have now changed their plans and have placed orders for equipment made by the Li River Plant.

Medium-High Capacity SPC Digital Long-Distance Switchboard Developed

91P60227C Beijing JISUANJI SHIJIE [CHINA COMPUTERWORLD] in Chinese No 25, 26 Jun 91 p 2

[Article by Xin You [2450 1429]: "New Breakthrough in Domestic Computer Applications in Communications Area: DS-30 Medium-High- Capacity Stored-Program-Controlled Digital Long-Distance Switchboard Developed"]

[Summary] The DS-30 medium-high-capacity stored-program-controlled (SPC) digital long-distance telephone switchboard developed by the Ministry of Posts & Telecommunications' (MPT) Institute 10 recently passed MPT-organized appraisal. The development of this exchange board is a new breakthrough for applications of domestic computer technology in the communications area, and fills a void in domestically made medium-high-capacity SPC digital trunkline exchange systems. It is the first domestically made digital exchanger to integrate multicomputer hierarchical control techniques and corresponding software with high-capacity network technology.

The switchboard includes a semiautomatic operator's system with voice- unit memory capability, a network subsystem, and a Chinese-character menu-driven intelligent terminal, and can be connected to ATME [automatic transmission measuring equipment] and to satellite and microwave systems. The software and hardware have a modularized design. Software is written in the PL/M high-level programming language, and consists of an operating subsystem (OS module, system supervisor module, diagnostic management module, and man-machine interface module) and applications subsystem (call-processing module, and maintenance management/

traffic/network supervision module). The hardware includes a single-board computer and monolithic microprocessor.

This switchboard has 1,000 lines (about 400-500 long-distance termini) in a basic module, a maximum capacity of 8,000 lines, and a maximum connection processing power of 120 KBHCA [thousand busy hour call attempts]. It is compatible with digital and digital/analog hybrid networks, and with all classes (C1, C2, C3, and C4) of long-distance switching centers.

New B-ISDN-Oriented Digital Communications Multiplexing System

91FE0635A Beijing RENMIN RIBAO in Chinese 7 Apr 91 p 3

[Article by He Huangbiao [0149 7806 1753] and Wang Guangren [3076 1639 0088]: "Two Professors at Qinghua Take Aim at Technical Problems in International Communications, Develop New Type of Digital Communications Multiplexing System"]

[Text] A digital communications multiplexing system with two types of modes—"reduced jitter positive justification technology and new multiplexing equipment for it" was successfully developed for the first time by Qinghua University professor Feng Zhongxi [7458 6850 3556] and assistant professor Zeng Lieguang [2582 3525 0342]. Its primary performance indices have a leading international status. This achievement received a 2nd-place state invention award in 1990.

Using digital communications to replace analog communications to achieve full digitization of information transmission exchange subscriber networks is a milestone in the modern communications era. Rapid growth in communications services now creates urgent demand for continual expansion of the capacity of communications circuits. The capacity of many international communications trunklines has now grown from a few 10 megabits per second to about 2,000 megabits per second. This is equivalent to expanding the number of telephone circuits from a few hundred circuits per trunkline to about 30,000 circuits. This expansion of capacity is achieved with digital communications multiplexing systems. Digital communications multiplexing systems have advantages like being capable of regenerating information, having powerful noise resistance capabilities, providing convenient information transmission and reception, being conducive to network management and operation, and so on. At the same time, however, they also bring in the harmful factor of multiplexing jitter that causes flickering of the picture elements in a graphic display which damages the quality of digital communications. Excessive multiplexing jitter can also create large amounts of errors in communications networks and thereby restrict the extension of communications networks.

At present, there are two main types of international regulations for multiplexing systems. One is a positive justification system and the other is a positive/zero/negative coding justification system. Due to existing technical limitations, neither of these two systems are sufficiently ideal for overcoming multiplexing jitter, which has affected the growth of fully digital communications networks and may restrict the major effort to push forward with integrated services digital networks [ISDN] and broadband integrated digital network [B-ISDN] operation. As a result, the Consultative Commission on International Telegraphy and Telephony [CCITT] made the requirement to develop modern digital communications networks the starting point and included further reductions in digital communications multiplexing jitter as a major international research topic. Experts and scholars in many industrially developed nations have suggested several methods for solution but none of these methods can be used because they do not conform to the two international standard systems stipulated by the CCITT.

Feng Zhongxi and Zeng Lieguang advanced by facing up to the problem and successfully developed a new type of digital communications multiplexing system. All of their functions and interfaces conform to international standards and regulations, so it is entirely suitable for use in international communications networks in China and other countries which adopt international communications standards. Even more gratifying is that it reduces multiplexing jitter to only 3.2 percent unit intervals, an index which not only satisfies the quality requirements of all types of modern information communications services but also satisfies the requirements of modern digital networks for broad regional coverage of digital networks, complex routing networks, large capacities, long distances, and frequent transmission and reception. It also solves the technical problem of reducing multiplexing jitter for which the CCITT requested research and solution. China has already designed and produced its own application-specific large-scale integrated circuits [ASICs] for this new system. Several products are already being used in actual projects and have extremely broad development prospects.

Domestically Developed ISDN Circuit Switching System

91FE0635B Beijing ZHONGGUO DIANZI BAO [CHINA ELECTRONICS NEWS] in Chinese 26 Apr 91 p 1

[Article by reporter Lin Feng [2651 2800]: "China Has Gained a Grasp of Key Technology for Integrated Services Digital Networks, Relying on Our Own Forces To Smash the Western Embargo"; cf. JPRS-CST-91-013, 20 Jun 91 p 5]

[Text] A modern communications technology which has long been restricted by a Western-nation embargo—integrated services digital network (ISDN) circuit switching systems—was recently successfully developed

by Shijiazhuang Institute 54 in the Ministry of Machine-Building and Electronics Industry (MMEI) and passed ministry-level examination and acceptance on 13 Apr 91.

ISDN is the premier development direction for communications networks. It uses a single communications network to provide high-quality voice, digital, facsimile, telex, visual telephony, and other services to subscribers. It can replace existing public switching telephone networks, public data exchange networks, telex networks, and other types of communications networks. At present, narrow-band ISDN from the industrially developed nations has already entered the application stage. ISDN is a high technology realm and has consistently been an item whose export and transfer to China have been controlled by COCOM. We have already imported 10 types of subscriber stored-program-controlled (SPC) exchanges and two Sino-foreign joint-venture large SPC production lines which lack ISDN functions and the related technology.

Without any technical information or software, MMEI's Shijiazhuang Institute 54 engineers began research on an experimental ISDN circuit switching system in April 1989. After 2 years of arduous work to attack key technical problems, they completed their assigned tasks. The experimental ISDN system is composed of an ISDN circuit switching simulator, an ISDN second-class network terminal, four ISDN first-class network terminals, and six digital telephones. On-site experiments, functional testing, and protocol testing have confirmed that the experimental ISDN system achieved the bureau's basic circuit switching functions and can provide subscribers with 64 kb/s unlimited circuit switching services and calling line identification, known as caller ID, and other service functions. It permits two types—basic rate and primary rate—of user access arrangements. Experts feel that the technical levels of this system have attained international levels of the mid-1980's and hold a leading status inside China.

Jiangxi-Fujian-Guangdong-Hunan DMW Network Completed

91FE0635C Beijing ZHONGGUO DIANZI BAO [CHINA ELECTRONICS NEWS] in Chinese 12 May 91 p 1

[Article by Sheng Xuan [4141 1357]: "Jiangxi Gives Priority to Development of Digital Microwave Communications"]

[Text] A digital microwave (DMW) communications network that will connect with a state first-level trunkline and link up 11 prefectures and cities in Jiangxi Province with nearby Fujian, Guangdong, and Hunan provinces will be completed in Jiangxi during the Eighth 5-Year Plan.

A domestically made (480 circuit) DMW circuit may also connect Jiujiang with Jingdezhen, Yingtan, and Shangrao at the end of June 1991. As the first phase (1992 target) of an MPT Eighth 5-Year Plan construction project to link Nanchang [Jiangxi Province] and Fuzhou [Fujian Province] with a state first-level (1,920-circuit) DMW trunkline, a DMW line will be built from Nanchang to Fuzhou [Jiangxi Province]. In addition, in the early part of the Eighth 5-Year Plan, Jiangxi will expand the capacity of the circuit between Nanchang and Ganzhou, connect it with Guangdong, and complete a circuit interconnection from Pingxiang to Hunan to form a DMW communications network connecting 11 prefectures and cities in Jiangxi Province with Fujian, Guangdong, and Hunan provinces that will provide an excellent communications environment for achieving an economic takeoff in Jiangxi during the Eighth 5-Year Plan.

Jiangsu's First Rural-Telephone DMW Crossbar-Switching Network Operational

91FE0635D Beijing DIANXIN JISHU [TELECOMMUNICATIONS TECHNOLOGY] in Chinese No 5, May 91 p 48

[Article by Jin Yuqi [6855 6877 3825]]

[Text] A rural-urban crossbar exchange network bureau employing digital microwaves as a transmission channel in Jiangsu Province's rural telephone network was placed into operation to connect Changshu City Bureau 62 with Meili Bureau 66 on 1 Jun 91. After testing of the network interconnection, the telephone connection rate between the bureaus reached 100 percent. The voice quality was clear and dialing was quick and accurate. It was warmly welcomed by the local governments and the popular masses.

This project was designed and built by technical personnel in the Changshu City P&T Bureau. The exchanges used in both bureaus are HJ-921A exchanges. Changshu has 8,000 city telephone switches [i.e. lines] and Meili has 1,000 rural telephone switches. The interface frameworks employ digital crossbar outgoing relays (SZCJ) and digital crossbar incoming relays (SZRJ), and the interface arrangement uses E and M line interfaces and R_2 digital circuit signals.

Success in this network interconnection project has provided experience in digital/analog compatibility in rural telephone networks and for a gradual transition to digital communications networks.

DMW Passive Diffraction Network Developed by Second Artillery Unit

91FE0635E Beijing RENMIN RIBAO in Chinese 21 May 91 p 3

[Article by He Huangbiao [0149 7806 1753]: "Gao Kunhua [7559 2492 5478] Overcomes Difficulties Blocking Wave Transmission, Microwave Passive Diffraction Network Successfully Developed and Placed into Operation"]

[Text] A highly efficient, portable, and inexpensive microwave passive diffraction network that does not require a power source has been successfully developed and placed into operation by engineer Gao Kunhua and others in the Engineering Design Institute of the PLA's Second Artillery Corps. The experts feel that this is a major accomplishment in the area of microwave communications engineering design in China and will substantially promote development of the communications industry.

Digital microwave communications are responsible for transmitting telephone, telegraph, images, computer communications, and other modern integrated communications services. Because the waves are transmitted directly, obstructing high mountains can create diffraction losses which make the signals extremely weak and unusable. The traditional method uses a relay arrangement to transmit the waves to a huge and complex active station built on the high mountain, after which they are retransmitted to the target. Because they involve long construction schedules, considerable engineering, and high construction costs, building a station in a location with terrible conditions can cost several million yuan.

The microwave passive network recently developed only requires installation of a portable metallic net similar to a volleyball net on a high mountain obstructing wave transmission; the new network can increase energy, strengthen signal directionality, magically jump the waves over obstructions and diffraction inflections, and achieve reliable communications. Adoption of this method does not require construction of lines and machinery buildings, nor does it require that people stay on duty. It costs only a few 10,000 yuan, equivalent to one in several tenths the cost of building a traditional station.

After the achievement was born, three of the new networks were installed on high mountain peaks in the Changbai Shan region at a savings of more than 2 million yuan compared to traditional methods. They have been operating for 3 years now with ideal results. Several dozen experts praised the very high applications value of this advanced achievement at the site and recommended that it be extended quickly.

Analysis, Testing of Mode-Partition Noise of Semiconductor Lasers in DS5 Fiber-Optic Transmission System

91P60203A Beijing TONGXIN XUEBAO [JOURNAL OF CHINA INSTITUTE OF COMMUNICATIONS] in Chinese Vol 12 No 3, May 91 pp 36-41, 88

[Article by Jiang Weijian [5592 5898 0256], Huang Shouhua [7806 1343 5478], Ph.D. candidate, Wuhan Institute of Posts and Telecommunications Sciences, and Ye Peida [0673 1014 1129]: "Experimental Research on Mode-Partition Noise of Semiconductor Lasers"; MS received 9 Oct 89, revised Oct 90]

[Abstract] Several methods for measuring the mode-partition noise [defined as the combination of mode-dependent optical losses, fluctuations in the distribution of radiant power or in the relative phases of the modes, and effects of differential mode attenuation] constant k of semiconductor laser diodes (LDs) are analyzed and compared. A novel statistical comparison measurement method, most closely suited to the actual conditions of LD operation, is presented.[1,2] The mode-partition noise of sample LDs is measured in 140 Mb/s [DS4 standard] and 560 Mb/s [DS5 standard] single-mode fiber-optic transmission systems, and results are compared to values predicted by the newly proposed method, with good agreement between the two.

The experimental system for testing mode-partition noise is depicted schematically in Figure 4 below. The power spectrum of the sample LDs is measured at modulation rates of 0, 140, and 560 Mb/s; center wavelength λ_c is 1.32 μm, longitudinal-mode separation $\Delta\lambda$ is 12 angstroms, and spectral-line half-width σ takes various values. The signal source employed puts out 140-560 Mb/s "0101" pulse trains and 2^7-1-bit-long NRZ PRBS (non-return-to-zero pseudorandom binary series) code. Measured values of k are shown in Table 1 below, while the experimental DS5 fiber-optic transmission system is shown in Figure 9 below. In this DS5 system, σ is 1.4 nm, $\Delta\lambda$ is 1.6 nm, λ_c is 1.52 μm, modulation signal length is 2^7-1, transmission rate is 560 Mb/s, and dispersion near the 1.55 μm single-mode-fiber wavelength is 17 ps/nm-km. Bit error rate (BER) is measured and plotted (Figure 11 below) against receiver input optical power P_r (in dBm) for various fiber lengths ranging from 2.8 km to 14.3 km; k is determined to be 0.447.

Table 1. Measured Values of Mode-Partition Constant k

LD	λ_c (μm)	$\Delta\lambda$ (nm)	2 σ (nm)	No. of longitudinal modes	k	
					140 Mbit/s	560 Mbit/s
No. 1	1.52	1.6	2.8	6	—	0.447
No. 2	1.54	1.4	2.0	5	0.457	0.492
No. 3	1.32	1.2	1.6	5	0.333	0.392

The results show that a 1 dB power loss generated by mode-partition noise occurs at a transmission range of 10.34 km, compared to the value of 11 km predicted by theory.[1]

References

1. Jiang Weijian, Feng Ronghui, and Ye Peida, "Improved Analysis of Dispersion Penalty in Optical Fiber Systems," OPTICAL AND QUANTUM ELECTRONICS, (22) 1990, 22-31.

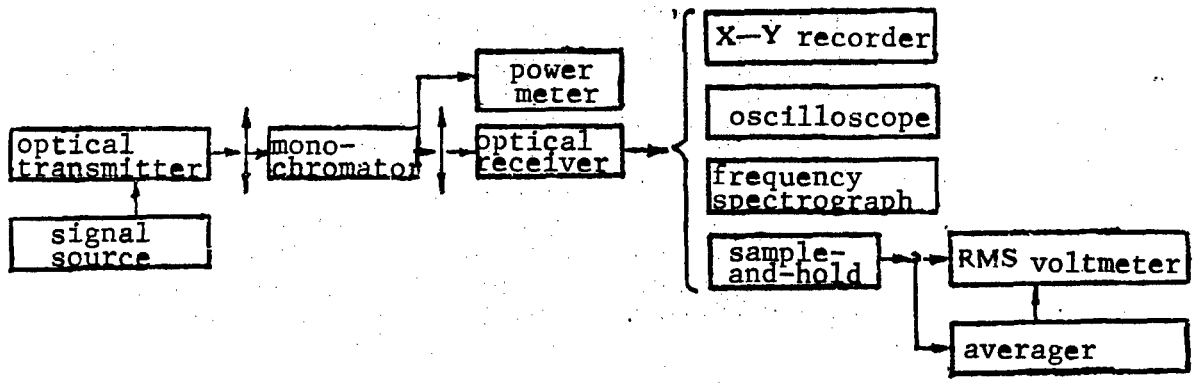

Figure 4. Schematic Diagram of System for Testing LD Mode-Partition Characteristics

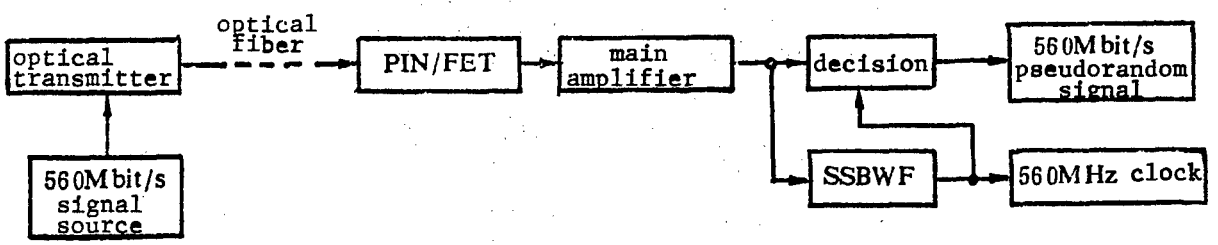

Figure 9. Schematic Diagram of Experimental Transmission System

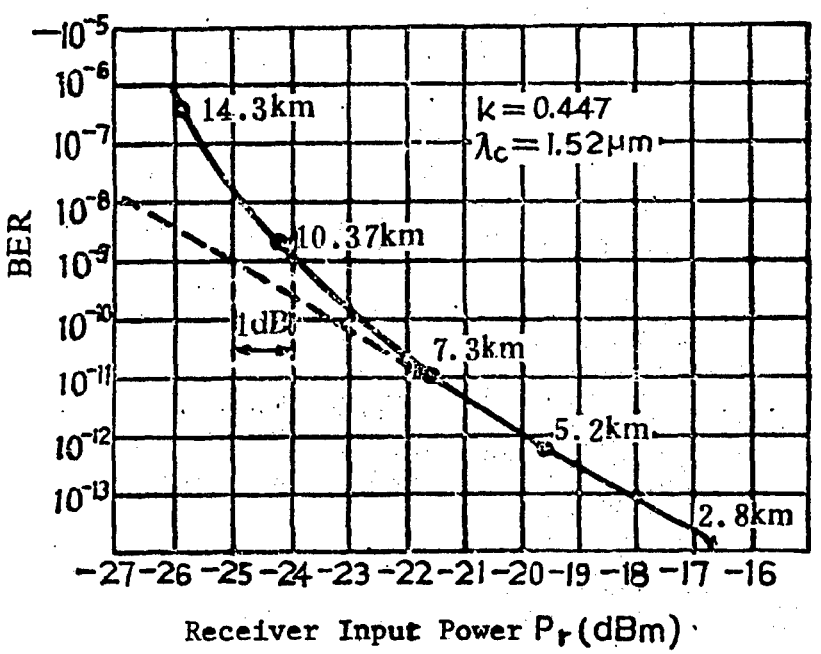

Figure 11. BER vs Receiver Input Power for Various Fiber Lengths

2. Jiang Weijian, Feng Ronghui, and Ye Peida, "Investigation of Mode-Partition Noise in Single-Mode Fiber Systems With an Improved Method," TONGXIN XUEBAO [JOURNAL OF CHINA INSTITUTE OF COMMUNICATIONS], Vol 12, No 3, 1991, pp 1-9.

3. K. Iwashita and K. Nakagawa, IEEE J. QUANTUM ELECTRONICS, Vol QE-18, No 12, December 1982, pp 2000-2004.

4. Y. Suematsu and K. Furuta, TRANS. IECE, Vol 60, 1977, pp 467-472.

5. H. C. Casey and M. B. Panish, "Heterostructure Lasers," Part A, New York: Academic Press, 1978, pp 110-186.

6. K. Ogawa and R. S. Vodhanel, IEEE J. QUANTUM ELECTRONICS, Vol QE-18, No 7, July 1982, pp 1090-1093.

Fujian Sanming-Yong'an DS4 Fiber-Optic-Cable System Marks 4 Months of Smooth Operation

91P60216A Beijing KEJI RIBAO [SCIENCE AND TECHNOLOGY DAILY] in Chinese 5 Jun 91 p 2

[Article by Ji Hongguang [1323 3163 0342]: "Domestically Made High-Capacity Digital Fiber-Optic-Cable Communications Equipment Operates Reliably"]

[Summary] The Fujian Province Sanming-to-Yong'an DS4 (140 Mb/s) [1,920 voice circuits] fiber-optic-cable digital communications system has now been operating smoothly for four months, indicating that the nation's independently developed high-capacity digital fiber-optic-cable communications equipment, meeting mid-eighties international standards, can satisfy requirements for long-haul trunklines. The Sanming-Yong'an system's equipment, which passed functional technical appraisal the other day, was provided by MPT's Institute 5 and by the Meishan Communications Equipment Plant.

According to MPT, China during the Eighth Five-Year Plan will construct a 20,000-km-long fiber-optic-cable communications network. Since it is advantageous as rapidly as possible to employ domestically made equipment, MPT assigned Institute 5 engineers the task of developing a DS4 fiber-optic-cable communications system, which was accomplished in the Seventh Five-Year Plan.

The Sanming-Yong'an line uses semi-directly-buried unattended repeaters, has an N:1 automatic protection switching ability, and can carry voice and FAX transmissions and teleconferencing [video/audio] communications. All of the system's technical indicators comply with International Telecommunications Union recommended standards.

Developments in Satellite Communications Reported

Nation's First Maritime Satellite Earth Station Operational

91P60217A Beijing KEJI RIBAO [SCIENCE AND TECHNOLOGY DAILY] in Chinese 4 Jun 91 p 1

[Article by Liu Zhenwu [0491 2182 2976]: "Nation's First Maritime Satellite Earth Station Operational"]

[Summary] The nation's first maritime satellite earth station, under construction since 1987, became formally operational on 3 June, marking China as the 20th nation to have such a facility. Located on the north side of Shangzhuang Reservoir in Beijing's Haidian district, the new earth station is equipped with two INMARSAT-system shore station equipment sets—one class-A (automatic/manually operated telephones, distress calling, etc.) set and one class-C (telex, data transmission) set—and two 13-m-diameter Cassegrain antennas, pointing to INMARSAT's Indian Ocean and Pacific Ocean satellites, respectively. The station can directly provide users with marine/air/ground mobile satcom services over two-thirds of the earth's surface; it has dedicated telephones for distress/safety communications and dedicated telex lines for direct link-up with the China Maritime Search and Rescue Center (RCC).

The INMARSAT organization, consisting of 65 member nations including China, utilizes four communications satellites to provide users—especially in underdeveloped areas—with mobile satcom services. INMARSAT representatives—as well as dignitaries such as Vice President Wang Zhen, NPC Standing Committee Vice Chairman Ye Fei, and representatives from the Ministry of Communications, the Ministry of Foreign Affairs, the [PLA] General Staff's Signal Corps Department, and the State Oceanography Bureau—attended the ribbon-cutting ceremony.

More on First Maritime Earth Station

91P60217B Beijing ZHONGGUO DIANZI BAO [CHINA ELECTRONICS NEWS] in Chinese 14 Jun 91 p 1

[Article by Liang Shu [2733 2118]: "Nation's First Maritime Satellite Earth Station Operational"]

[Summary] The Beijing coastal station's two standard equipment sets provide service to Pacific Ocean and Indian Ocean users, respectively. Via two 7 GHz digital microwave transmission systems, the station can provide access to telephone and telex public networks and to Ministry of Communications dedicated long-distance networks. For each ocean area served, the station provides 20 ship-to-shore telephone lines, 20 ship-to-shore telex lines, 16 shore-to-ship telephone lines, 20 shore-to-ship telex lines, two distress dedicated telephone lines, and two distress dedicated telex lines directly connecting

to RCC. The station can provide communications services for up to 16,000 mobile stations.

Domestically Made Chengdu Earth Station Formally Operational

91P60217C Chengdu SICHUAN RIBAO in Chinese 13 Jun 91 p 1

[Article by Gong Jianping [7895 1696 1627]: "Chengdu Satellite Earth Station, Wuhan-Chongqing Microwave Circuit Formally Put Into Operation"]

[Summary] The highest-capacity communications project in terms of lines going out from this province—the Wuhan-Chongqing microwave line—and the nation's first domestically made satellite earth station, the Chengdu Satellite Earth Station, passed MPT-organized acceptance check on 12 [June] in Chengdu, and are thus formally operational. The microwave line and the earth station together will add 140 percent to the number of out-of-province circuits.

The Wuhan-Chongqing microwave line, 1,053.5 km in length, has 28 microwave stations, and was built with an aggregate investment of 99,755,000 yuan. It will be put on line with various fiber-optic-cable and microwave networks in the area.

The Chengdu Satellite Earth Station, the province's first satellite earth station, is also the nation's first independently designed and developed satellite earth station. Via direct satellite hook-up, this station can be linked to the Beijing, Guangzhou, Lhasa, Urumqi, and Shanghai earth stations. The station currently has 120 telephone circuits, but MPT is arranging for capacity to be expanded to 900 circuits.

Technical Details of China's First Pulsed Reactor Reported

91FE0483A Chengdu HE DONGLI GONGCHENG [NUCLEAR POWER ENGINEERING] in Chinese Vol 12 No 1, Feb 91 pp 2-11, 25

[Article by Xia Xianggui [1115 4382 6311], Wang Zisheng [3769 2737 3932], Lu Shaoji [7120 4801 2623], Ruan Guixing [7086 2710 5281], and Li Dazhong [2621 6613 1813] of the Nuclear Power Institute of China [formerly Southwest Institute of Reactor Engineering Research & Design], Chengdu: "China's First Pulsed Reactor"; MS received 17 Sep 90]

[Text] Abstract: China's first pulsed reactor is a small pool-type research reactor using $UZrH_{1.6}$ rods as its fuel-moderator elements. The core is cooled by naturally circulating light water and the reflector is made of graphite. The reactor has a very large prompt negative temperature coefficient. It not only can operate in steady state, but also in unique pulsing mode and square-wave mode. The nominal power of the reactor in steady-state operation is 1,000 kW and the mean core thermal neutron flux is 1.4×10^{13} n/(cm^2-s). When three units of prompt positive reactivity (i.e., $2.1 \times 10^{-2}\Delta K/K$) are inserted into the core in the pulsing mode, reactor peak power is approximately 3,420 MW and its peak neutron flux is approximately 6×10^{16}n/(cm^2-s). The prominent advantages of this pulsed reactor include inherent safety, economy, and versatility. This reactor reached its critical state on 22 July 1990 and has since been in test operation.

Key Words: pulsed reactor, uranium and zirconium hydride, pulsing operation, prompt negative temperature coefficient, inherent safety.

I. Introduction

China's first pulsed reactor was designed and constructed by the Nuclear Power Institute of China (NPIC). All the equipment and instrumentation were domestically developed and manufactured; work began in January 1987. In December 1989, the installation of the reactor and testing of individual systems were completed. The testing of the overall system (nonnuclear) was completed in January 1990. In May 1990, the State Environmental Protection Bureau approved the final environmental impact report. In the same month, after passing a nuclear safety review, system testing inspection, operator qualification accreditation, and emergency evacuation plan review, the Nuclear Safety Administration issued a license to load fuel for the first time. Under the supervision of the Nuclear Safety Administration, nuclear fuel was loaded for the first time on 20 July following the operating and testing procedures. On 22 July, it reached the cold critical state for the first time. Afterward, it went into steady-state operation. The successful completion of the reactor provides the necessary conditions to meet the growing demand for nuclear power, and also fills a void in research reactor in China. This is a breakthrough in nuclear technology for NPIC.

During the initial design stage, we encountered numerous technical hurdles. There were three major issues, i.e., development of the theoretical computation program; design and manufacture of the $UZrH_{1.6}$ fuel-moderator elements; and pulse emission, measurement of pulsing parameters and development of instrumentation for the measurements. To overcome these technical hurdles, we organized technical people in over 50 experimental programs. After a few years of exploration and experimentation, these hurdles were overcome one by one.

The pulsed reactor we built is a prototype for verification purposes, and is used to finish a series of experiments. The principal objectives are: 1) to understand its physical and thermal properties, confirm the theory and verify the design; 2) to test key equipment, instrumentation, and fuel elements as the reactor runs; 3) to study the operation and experimental technique associated with this reactor; and 4) to provide experimental data and first-hand information for the design of a commercial pulsed reactor.

II. Design Features

The pulsed reactor is a pool-type research reactor using $UZrH_{1.6}$ as its fuel-moderator element. Its advantages include inherent safety, economy, and versatility. It is especially suitable for commercial use.

1. Inherent Safety

The reactor was designed to use zirconium hydride ($ZrH_{1.6}$) as the moderator. The moderator and fuel are mixed homogeneously to form a fuel rod. The core has a very large prompt negative temperature coefficient, as high as $-(1.1\text{-}1.2) \times 10^{-4}$ ($\Delta K/K$)/°C. When a fixed step of positive reactivity is introduced to the core or when some positive reactivity is introduced to the core by mistake to push reactor power and fuel temperature steeply upward, the temperature of the homogeneous moderator-fuel mix also rises without any delay. The prompt negative temperature coefficient produces negative reactivity inside the reactor. The higher the element temperature, the larger the negative reactivity becomes, until the positive reactivity introduced to the core is completely canceled. Thus, the reactor power is brought back to its steady-state value in a safe and timely manner. This safety feature does not require the activation of any electromechanical protection system or manual intervention. Therefore, it is inherently safe. This is why this type of reactor can safely run in the pulse mode, exceeding prompt criticality up to several units of positive reactivity. Hence, it is called a pulsed reactor.

In addition, uranium zirconium hydride has excellent compatibility with fission gases, approximately 3-4 orders of magnitude higher than that of uranium

dioxide. This material also has excellent chemical stability. Its reaction with water is also very weak even when heated samples are immersed in water or when it is boiled in high-temperature high-pressure water over long periods of time.

The reactor uses an under-moderated core design. The volume ratio of fuel-moderator elements to water is approximately two-thirds to one-third. When there is less water in the core, or cavity in the active area, the reactivity of the core is reduced to further enhance safety.

We have done an accident analysis which shows that the peak core element temperature, surface temperature of element cladding, and peak stress on element cladding are below the design values under different conditions and the cladding will not be damaged to jeopardize reactor safety. The details of this analysis are given in an article entitled "Pulsed Reactor Accident Analysis," elsewhere in this issue.

The results of environmental impact calculations are shown in Table 1.

Table 1. Environmental Impact Results

Operating condition	Effective dose equivalent	Calculated value	Standard limit (GB6249-86)
Normal	Individual effective dose equivalent, mSv/a	9.93×10^{-4}	0.25
	Collective effective dose equivalent, man-Sv/a		
	Within 5 km	7.14×10^{-4}	—
	Within 80 km	1.14×10^{-3}	—
Baseline accident*	Individual effective dose equivalent (8 hours after accident at 130 m), mSv	5.12×10^{-2}	Dose standard per major accident <5
	Collective effective dose equivalent (30 days after accident), man-Sv/a		
	Within 5 km	1.38×10^{-2}	—
	Within 80 km	2.58×10^{-2}	2×10^{4}

* A baseline accident involves loss of water, simultaneous damage to the highest-power element (2 percent of reactor power), and failure of filter and iodine remover.

2. Good Economy

The reactor has a compact structure and the core is cooled by natural circulation of pool water. Even during complete power failure or loss of the main cooling system, the residual heat of the core can be completely conducted out by natural circulation. Therefore, it does not require an emergency core cooling system or provision of two independent power supplies for the main cooling system. Thus, the system is relatively simple. Because of its inherent safety, the requirements on nuclear- safety-related facilities can be reduced to lower the construction cost. Moreover, it is simple to operate and maintain. It requires fewer people and lower cost to operate; it is very economic as a whole.

3. Versatility

Commercial pulsed reactors not only can be used for research purposes, such as neutron activation analysis, neutron photography, radiation experiments, isotope production, teaching and training, but also can undertake tasks that other research reactors cannot perform due to the unique pulsing mode, including conducting instantaneous radiation experiments on fuel elements, studying safety and dynamic characteristics of reactors, investigating instantaneous radiation effects on electronic devices, and studying certain dynamic processes by pulsed neutron photography. Hence, pulsed reactors can be widely used in industry, agriculture, medicine, environmental protection, surveying, archaeology, justice, crime, and food processing.

III. Major Design Parameters

The major design parameters of the reactor are shown in Table 2.

Table 2. Major Design Parameter for the Pulsed Reactor

1. Rated steady-state parameters	
Steady-state rated power, kW	1,000
Load under rated condition, kg (^{235}U)	3.497 (86 elements)
Mean core thermal neutron flux, n/cm^2-s	1.4×10^{13}
Mean core fast neutron flux, n/cm^2-s	2.4×10^{13}
Mean core power, W/cm^3	17.02
Natural circulation through the core, t/h	27.43
Mean core flow rate, m/s	0.122
Mean core inlet/outlet temperature, °C	35/66.3

Table 2. Major Design Parameter for the Pulsed Reactor (Continued)

Pool water circulation flow, t/h	86
Maximum element core temperature, °C	480
Maximum element cladding temperature, °C	135
Mean heat flow density, W/cm^2	27.43
MDNBR [Minimum departure from nucleate boiling ratio]	3.28
Core life, MW-d	150
2. Prompt negative temperature coefficient(ΔK/K)/°C	-1.1 x 10^{-4} (operating temperature)
3. Cold state parameters	
Critical mass, kg (^{235}U)	2.142 (54 elements)
Reserve reactivity, 10-^{2}ΔK/K	6.717
Total control-rod value, 10^{-2}ΔK/K	11.373
4. Pulse parameters	
Maximum inserted prompt positive reactivity, units	3
Pulsed peak power, MW	Up to 3,420
Pulsed peak flux, n/cm^2-s	Up to 6 x 10^{16}
Instantaneous energy released, MJ	33.07

IV. Description of the Reactor

This prototype reactor is composed of the reactor body, coolant and purification system, measurement, control and protection system, dose monitoring system, ancillary system, and experimental facilities.

The core of the reactor is located at the center of the pool bottom. It is supported by a frame which is tied to the bottom of the pool, as shown in Figures 1 and 2. It is surrounded by a cylinder of reflector layers, consisting of a graphite reflector layer and lead shielding layer from inside out. Outside this cylinder is the water shield layer. The stainless-steel pool is surrounded by reinforced concrete. There are axial graphite reflectors at the top and bottom end of the fuel core, sealed in the fuel cladding. Above the core, there is a 5-m-deep light water layer of shield. Over the water surface, there is a negative pressure zone which is not filled with water to avoid the diffusion of radioactive ^{41}Ar into the reactor building.

The core components are laid out concentrically in seven circles. From inside out, the number of elements in each circle increases by six. There are a total of 127 grid elements (numbered in clockwise order). The central vertical tube is located in the middle. The four control rods (i.e., adjustment rod C_{10}, pulsing rod C_4, safety rod D_{10} and compensation rod D_1) are located in circles C and D in pairs symmetrically perpendicularly to each other. The outside circle has 35 graphite elements and one neutron source element. The remaining elements are 86 uranium zirconium hydride fuel-moderator elements. The core is also equipped with a number of neutron flux and temperature measuring devices. The layout is shown in Figure 3.

The coolant enters the inner cylinder from the bottom and then flows upward across the upper and lower grid plates to form a natural circulation loop to cool the core.

There is a bridge over the pool across the core. It is used to support four control rod drive mechanisms and to secure the central vertical tube. There are three pool cover plates on either side of the bridge, together with the bridge itself, to seal the top of the pool completely.

There is an injector above the core to spray coolant over the core when it runs. It forms a disturbance zone in the rising water layer above the core to slow down the rise time of the radioactive ^{16}N gas in order to lower the dosage at the top of the core.

The reactor can operate in manual, pulsing, and square-wave modes. The mode of operation is determined by the position of the mode-selection switch on the control panel. The control desk contains all the necessary nuclear instrumentation and control and protection circuits. On the right side of the control desk, there is an alarm screen, core neutron flux density instrumentation panel and process instrumentation panel. Ergometrics has been considered in the design of the control desk. All displays and recorders are located in places that are easy to read. All switches and buttons are installed at places that permit easy access and operation. Furthermore, parameters critical to the operation and safety of the reactor are displayed and indicated in order to avoid any confusion caused by mixing these signals with other relatively unimportant signals.

1. Reactor Body

(1) Reactor pool

The pool has a stainless-steel surface and an external concrete shield. The inlets and outlets of various systems are scattered around the wall. There are two symmetrically installed lifts for temporary underwater storage of fuel elements and control rods. In addition, there is a sealed box for storage of damaged fuel elements, a storage rack for the box, and an underwater fuel-element inspection device.

The concrete shield has two layers. the lower layer is 3.4 m high (from the floor of the reactor building) and the upper layer is 3.24 m high. They are octagonal in cross section. The top of the reactor has an octagonal cantilever platform for assembly, testing, and experimentation.

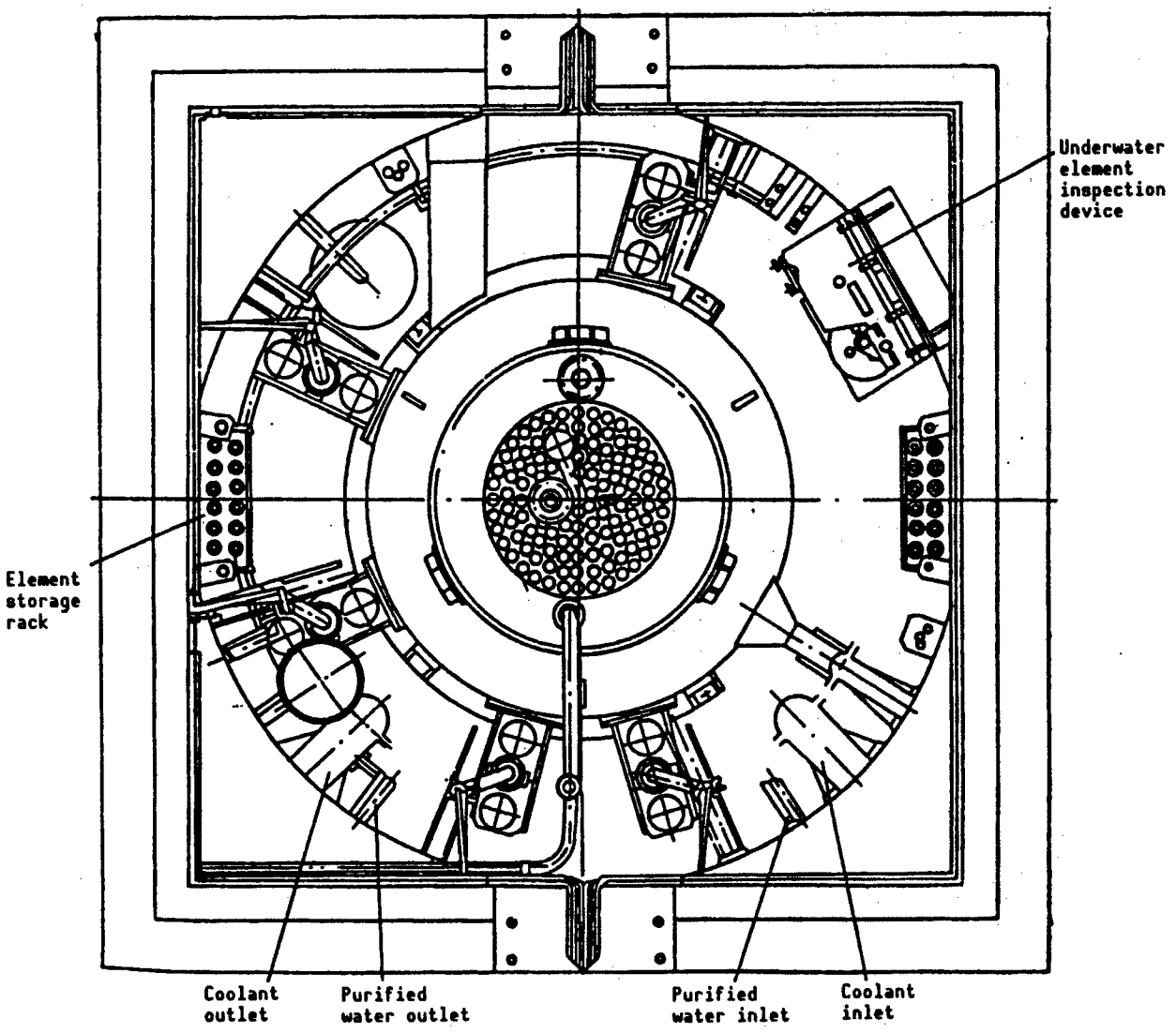

Figure 1. Cross Section of the Pulsed Reactor

(2) Reactor internals

As shown in Figure 4, there are three structural components in the reactor, i.e., the inner cylinder, the reflector cylinder, and the support. The inner cylinder is made of a special aluminum alloy. the upper grid is on top, the lower grid is in the middle, and the safety plate is on the bottom. The upper grid has 127 38-mm-diameter holes. In addition to securing fuel elements and control rods horizontally, they also act as the outlet for the naturally circulating coolant. Furthermore, there are two symmetric triangular openings. Each triangular opening takes up the space of one D-ring hole and two E-ring holes. When fuel elements are inserted into these holes, the horizontal position is fixed by the element locator at the head. After fuel elements and element locators are removed, a 61-mm-diameter aluminum pipe can be inserted as an off-center experimental cavity. The lower grid also has 127 corresponding holes to support the elements and to serve as the coolant inlet. The weight of the elements is entirely supported by the lower grid. The safety plate is there to prevent control rods from falling out of the core to ensure reactor safety.

The reflector cylinder has a sealed graphite layer and a lead shield. It also has radial and tangential channels. Its top provides a ring to install the rotating sampling rack. The support for five ionization chambers is welded to the outer wall. The reflector cylinder is filled with helium to improve the thermal conduction property and to inspect the quality of the last weld to ensure the hermeticalness of the vessel.

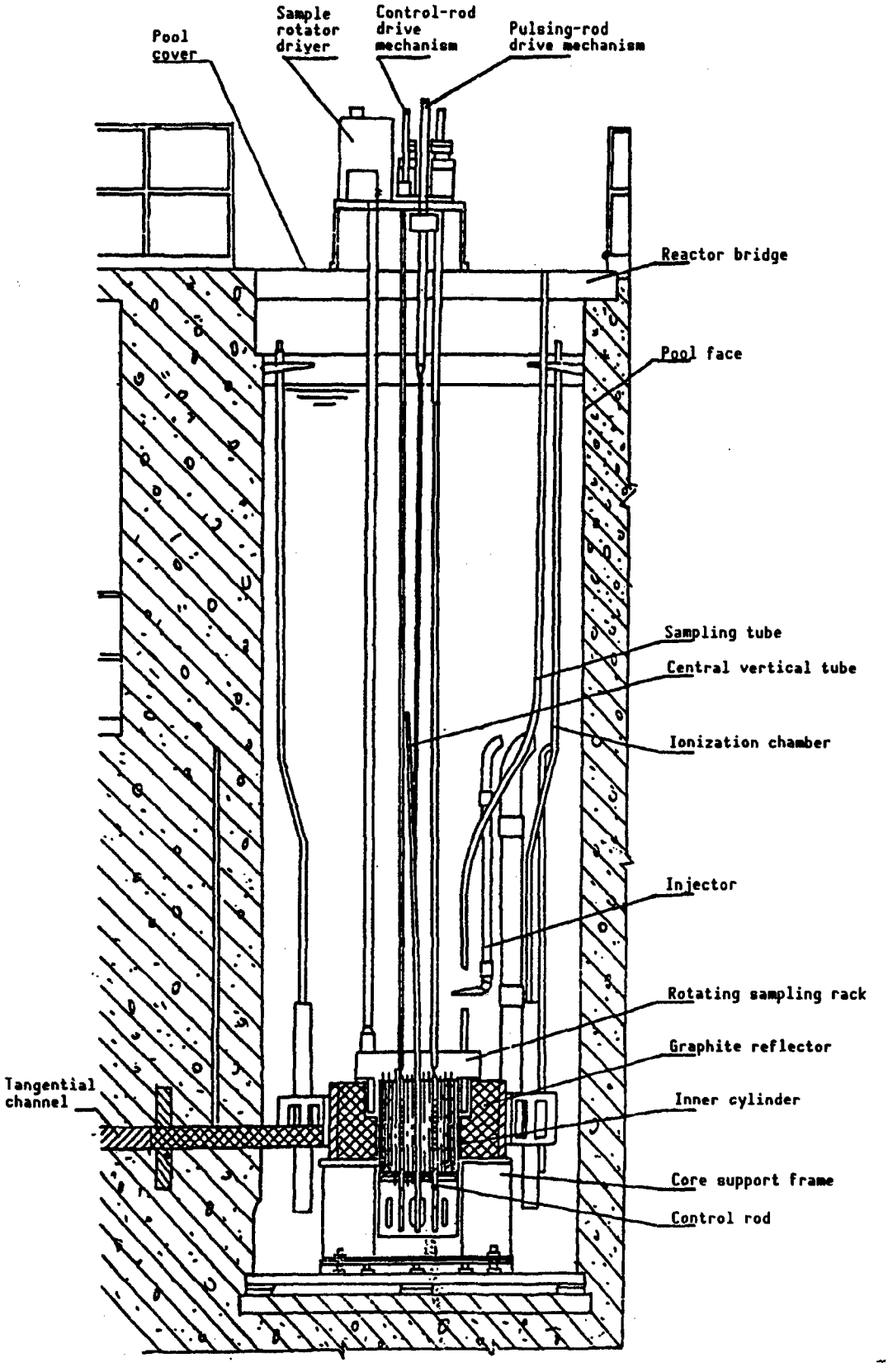

Figure 2. Longitudinal View of the Pulsed Reactor

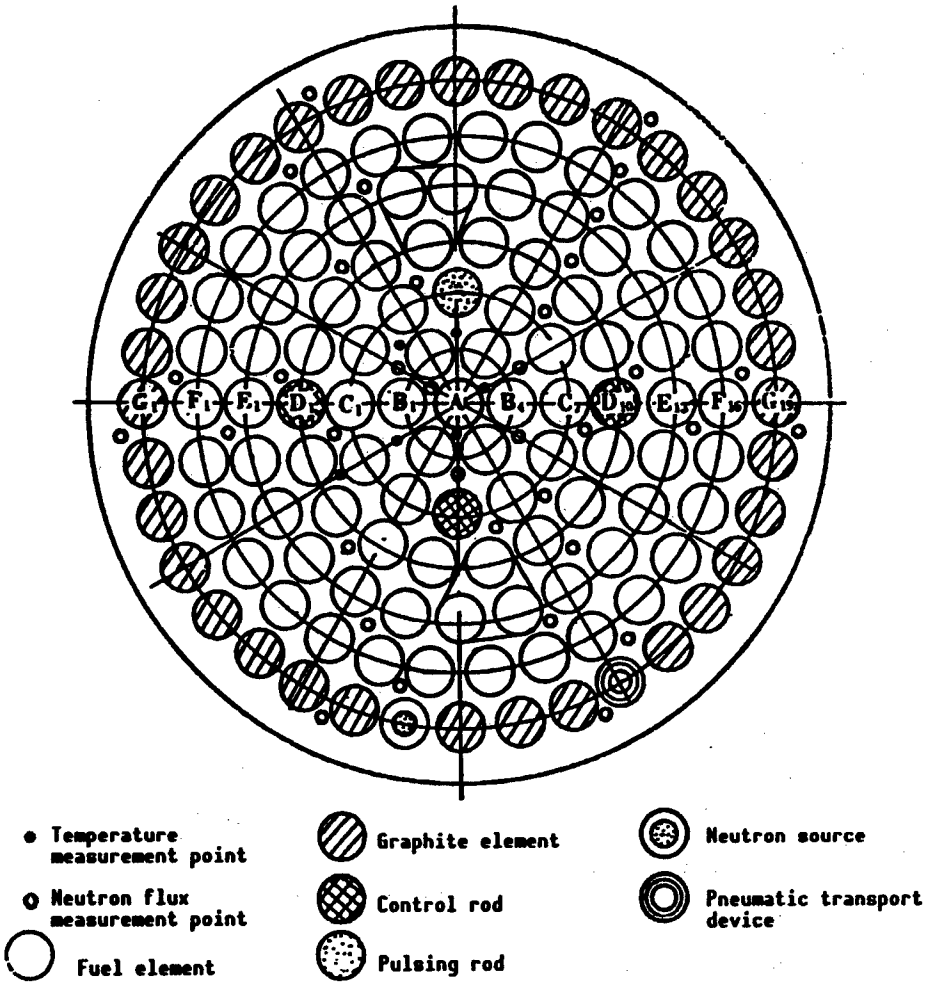

Figure 3. Core Layout

(3) Fuel elements

Fuel elements are divided into two types, i.e., standard and instrumentation. The instrumentation type of fuel element is used to measure fuel-core temperature and cladding temperature.

Figure 5 shows the structure of the standard fuel element. The cladding is made of stainless steel. Each fuel element contains three pieces of $UZrH_{1.6}$. There is a zirconium alloy rod at the center of the core. A piece of graphite is placed above and below the core as an axial reflector. In order to compensate for radiation expansion of the fuel and graphite during use and the axial thermal expansion difference of the case, a suitable axial gap is left above the upper graphite block. Similarly, a radial gap is left between the core and the case. After the upper and lower end are welded, it is filled with helium.

In order to continuously monitor the operating temperature of the fuel to ensure reactor safety and to verify the nuclear thermal design, this reactor is equipped with two fuel-core thermometric devices. The device structure is different from that of a standard fuel element. The major difference is that the middle fuel pellet has three holes for insertion of three armored thermocouples. The device structure is shown in Figure 6.

In order to monitor the cladding operating temperature to verify the thermal nuclear design, the reactor is equipped with an element with cladding thermometric capability. Its structure is identical to that of a standard element. The difference is that the outer wall has three armored thermocouples to measure the operating temperature of the cladding. These thermocouples are welded on the outer cladding wall, corresponding to the centers of the three fuel pellets.

(4) Steady-state control rod

Figure 7 shows the structure of the steady-state control rod (safety rod, adjustment rod, or compensating rod). The cladding is made of stainless steel and contains 10

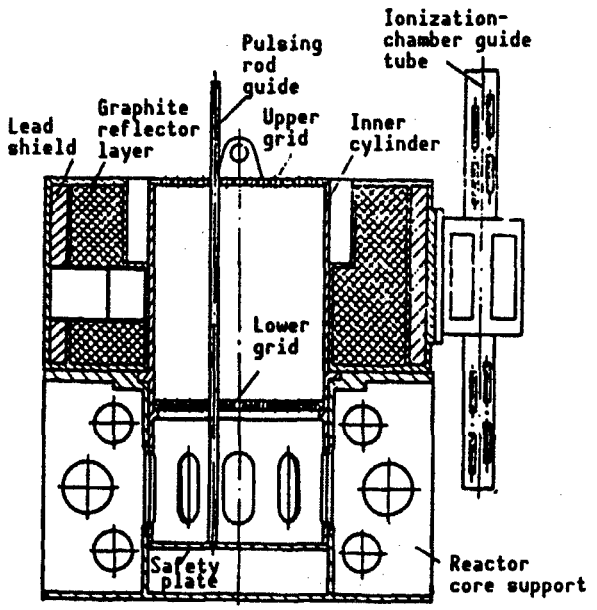

Figure 4. Reactor Internals

neutron-absorbing B_4C pellets. Its axial position is that the lowest position of the steady-state rod is at the same level as the active section of the core. The lower three $UZrH_{1.6}$ fuel pellets belong to the following section. This section is at the same level as the active core section when the steady-state control rod is at its highest position. The cladding is filled with helium.

(5) Pulsing rod

The function of the pulsing rod is to introduce several units of positive reactivity by ejecting the pulsing rod out of the core within a short time via its drive mechanism in order to achieve pulsing operation.

Figure 8 shows the structure of the pulsing rod. It is primarily composed of an upper cavity, a neutron-absorbing section, and a lower cavity. The neutron-absorbing section, consisting of 10 pieces of B_4C, is used to control reactivity. Its axial position is determined by the fact that the neutron-absorbing section is at the same level as the active section of the core when the pulsing rod is at its lowest position. The cladding is made of aluminum alloy.

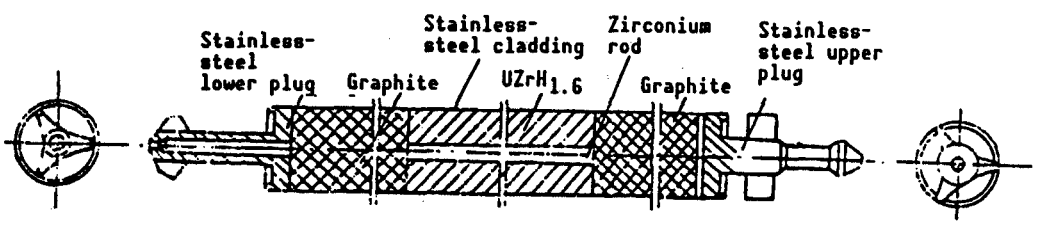

Figure 5. Schematic Diagram of the Pulsed Reactor Fuel Element

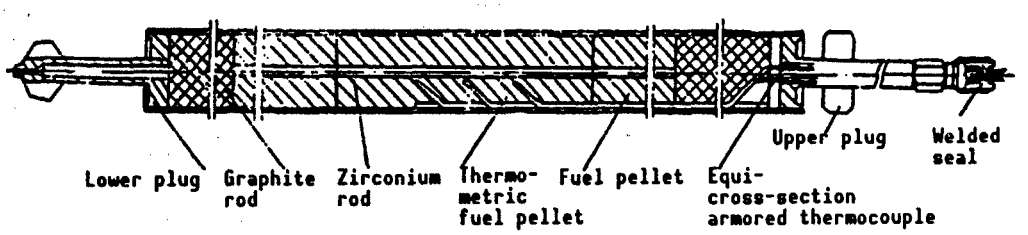

Figure 6. Schematic of Fuel-Core Thermometric Device

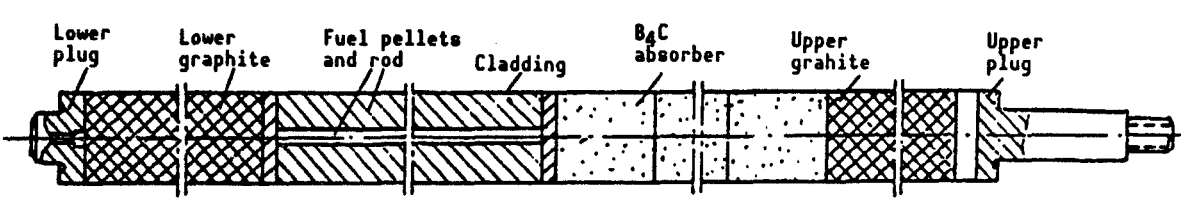

Figure 7. Schematic Diagram of the Steady-State Control Rod

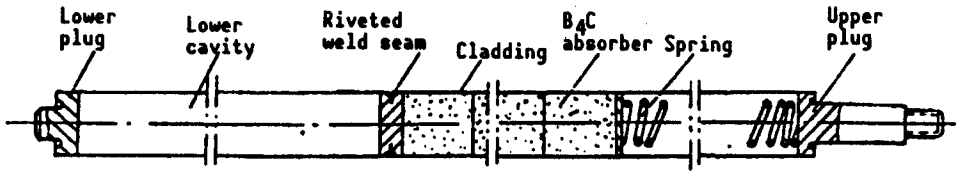

Figure 8. Schematic Diagram of the Pulsing Rod

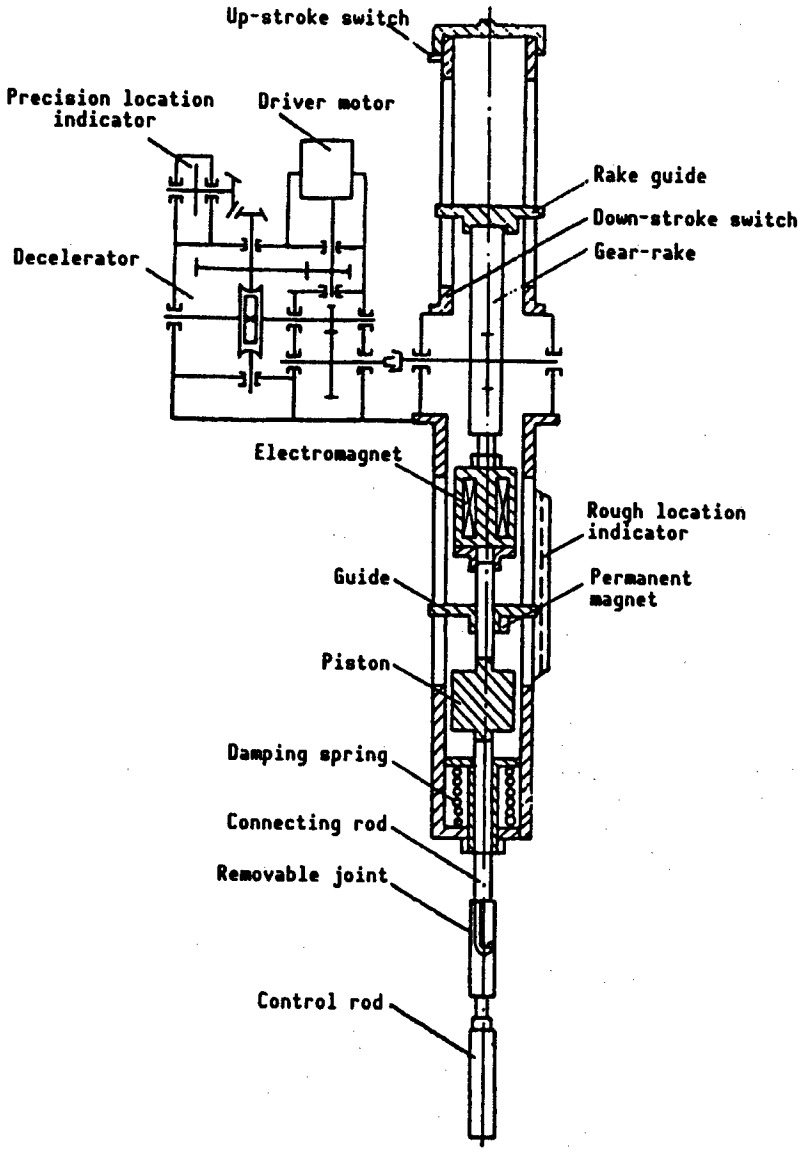

Figure 9. Steady-State Control-Rod Drive Mechanism

(6) Steady-state control-rod drive mechanism

The three steady-state control rods are driven by gear and rack mechanisms. The position of the rod is controlled by a spring-loaded tube. The rod speed is 500 mm/min and the entire insertion duration is less than or equal to 0.8 second. When the electromagnet is powered, it sticks to the anchor and the entire driver becomes one

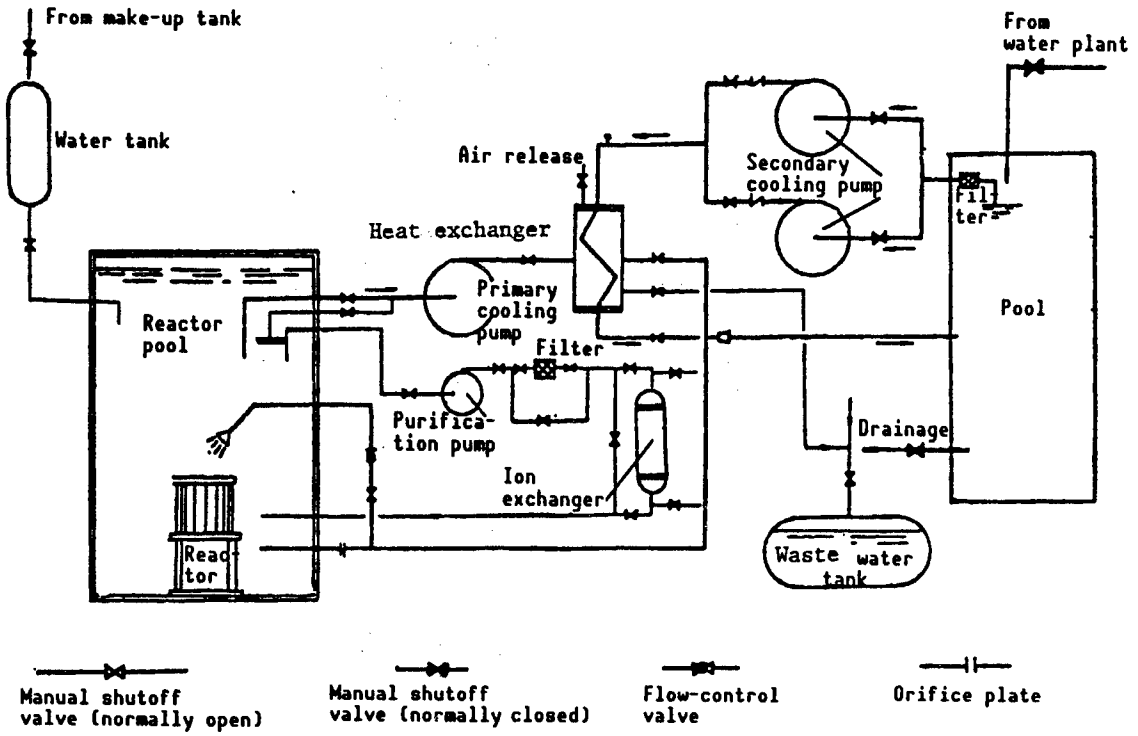

Figure 10. Flow Diagram of Coolant System and Purification System

body. The control rod moves up or down depending on whether the motor runs forward or backward. When the electromagnet loses its power, it disengages with the anchor. The control rod falls rapidly into the core by gravity. Control-rod structure is shown in Figure 9.

2. Coolant System and Purification System

The coolant system includes a primary and a secondary system.

The primary system is an open loop which transfers heat from the reactor pool by forced circulation in order to maintain the pool temperature at below 45°C. It consists of a centrifugal pump, a heat exchanger and several valves and pipes. The flow diagram is shown in Figure 10. The inlet and outlet pipes enter the pool at 3.7 m from the bottom. The inlet is 0.7 m from the pool bottom and the outlet is 2.7 m from the bottom. The entire system is installed in a room 3 m above the reactor core. In the event of an accident which causes the fracture of the primary pipe, the core remains submerged and the safety of the reactor will not be affected. The heat exchanger is a water-water type of tube exchanger made of stainless steel. The primary pump is a stainless steel centrifugal pump. The system is equipped with pressure gauges, thermometers, and flow meters to monitor its operation and to measure the thermal power of the reactor.

The purification system is also an open-loop system which can operate intermittently or continuously. Its function is to remove both soluble and insoluble impurities in the pool water to maintain the quality of water within certain specifications. This is required to lower coolant radioactivity, reduce corrosion rate of reactor materials, particularly fuel elements, and maintain pool water quality. The system is composed of a stainless-steel purification pump, a filter, an ion exchanger, several valves, and a number of pipes. Its flow diagram is also shown in Figure 10. The system is equipped with a flow meter, pressure gauge, temperature gauge, pH meter, and conductivity meter to monitor its operation and to measure water-quality-related parameters.

3. Measurement and Control Protection System

The measurement and control protection system consists of the following eight subsystems: 1) excore nuclear measurement system; 2) incore nuclear measurement system; 3) incore/excore thermometric system; 4) control system; 5) power adjustment system; 6) protection and interlock system; 7) alarm system; and 8) control-rod position display system. These systems are described in other articles in this special issue and will not be repeated here.

4. Dose Monitoring System

The dose monitoring system monitors gamma radiation, radioactive gases and aerosols, and fuel-element damage.

5. Ancillary Systems

The ancillary systems consist of a power supply (including normal power supply, backup power source and lighting system), communications system, ventilation system, water make-up system, radioactive waste-water collection and storage system, normal water and sewage system, fuel loading and storage system, and fire prevention system.

6. Experimental Facilities

A commercial pulsed reactor has experimental facilities such as hot columns, radial and tangential channels, central vertical channels, off- center vertical channels, "running rabbit" devices, rotating sample rack and driver box, etc. Since this reactor is not for applied development use, it is only equipped with horizontal tangential and central vertical channels.

The horizontal tangential channel has a simple setup which is used to measure parameters to verify theoretical nuclear calculations. The channel consists of inner and outer segments. The inner segment is sealed inside the reflector cylinder. The outer segment goes through the concrete shield and the wall of the reactor pool. It is filled with several sections of shielding materials, and is vented above the pipe.

V. Conclusion

A pulsed reactor is attractive due to reasons such as its inherently high safety, minimal environmental pollution, and low construction cost. Over 60 such reactors have been built in more than 20 countries, and are called TRIGA [training, research, isotope-production reactor, General Atomics design] reactors abroad. In recent years, countries such as Canada and the United States have been developing this kind of small reactor into a small power plant for supplying electricity and low-level heating. Although we have built our first pulsed reactor, we still have a long way to go; there are many tasks to be completed.

4-Megavolt Accelerator Laboratory Completed

91P60222A Shanghai JIEFANG RIBAO in Chinese 8 Jun 91 p 1

[Article by Jia Baoliang [6328 1405 5328]: "4-Megavolt Accelerator Laboratory Completed in Shanghai"]

[Summary] After five years of labor, scientists and engineers at the CAS Shanghai Institute of Nuclear Research have basically completed a state-of-the-art 4-MV accelerator laboratory. This static-electricity accelerator lab, which will furnish a means for furthering cutting-edge nuclear technology applications, as well as aiding research in life sciences, materials science, and earth sciences, includes advanced equipment and technology imported from abroad, such as an ultra-high-vacuum target chamber, a scanning proton microprobe system, a particle-excitation X-ray analysis dedicated beam-current line, and other experimental apparatus. To date, the new accelerator has successfully operated for almost 10,000 hours, and has been employed in over 30 research projects, of which almost half were major international cooperative efforts. Over 150 scholarly papers describing these projects have been published in domestic and foreign journals.

Analysis of Waves Generated by Explosion Near the Water Surface

91FE0560A Beijing LIXUE YU SHIJIAN [MECHANICS AND PRACTICE] in Chinese Vol 13 No 2, Apr 91 pp 47-49; MS received 31 Dec 89

[Article by Li Runshan [2621 3387 3790] and Yi Jiayu [2496 0857 6877] of Naval Institute of Engineering Design and Shen Guoguang [3088 0948 0342] of Tianjin University, a project funded by the National Natural Science Foundation: "Analysis of Waves Generated by Explosion Near the Water Surface"]

[Text] Abstract: Experiments were conducted to measure the waves and hydrodynamic pressure generated by explosions equivalent to 0.1 to 32 kg of TNT near or in contact with the water surface. This paper introduces our results and preliminary investigation of the wave-making mechanism.

Key Words: wave making by explosion, hydrodynamic pressure, explosion height.

When an explosion originates near or at the water surface, in addition to generating an intense shock wave, huge surface waves can be produced which may cause significant damage to ships and coastal buildings. Hence, since the advent of nuclear weapons, wave making by explosion has been a hot research topic. A number of reports have been published since the 1960's. However, there are two areas of weakness: One is that more work has been done on underwater explosion and not enough on above water explosion; the other is that very little work has been published regarding the wave-making mechanism and actual measured data due to difficulties in theoretical study and limitations in measuring techniques. In recent years, we have performed explosion experiments near and at the water surface in order to investigate the wave-making mechanism and the laws governing its propagation and its characteristics.

1. Formation of Waves From Explosion Near the Water Surface

When an explosion is detonated over the water surface, a great deal of energy is instantaneously released. This energy is rapidly transferred to the neighboring air and water. The expansion of the explosion product and the shock wave from the fireball put pressure on the water surface to form the initial crater (see Figure 1). Furthermore, they also produce an out-going surface wave, i.e., the initial wave-making phenomenon. Afterward, because the outward motion of the fluid is partially suppressed, the water near the crater moves toward the

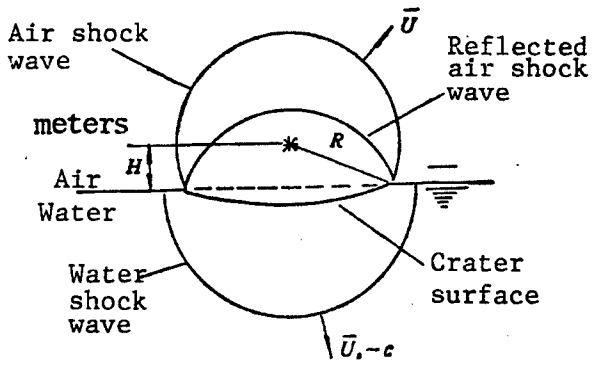

Figure 1. Waves Associated With Near-Water-Surface Explosion

center due to gravity. On top of it, there is a tremendous upward draw because the air is thin from gas diffusion over the crater, which provides an upward velocity for the water in the crater. The water rises as a column and splashes down. For instance, when an 8-kg explosive detonates at the water surface, the water column rises up to 16 meters. Approximately two seconds after explosion, the column falls to form a crater for the second time and makes even larger waves. These are the so-called follow-up waves.

Our experimental results show that the major factor affecting the crater, water column and wave is the explosion specific height. As the specific height increases, the crater becomes shallower, the water column lower and waves smaller.

As for underwater explosion, there is almost no water splashing. The water column is a slender cylinder, going vertically upward and reaching as high as several dozen meters (with only a few hundred grams of TNT). However, it is mostly fine water beads and mist and has no significant effect on the surface wave. Waves are primarily produced by the underwater shock wave and the interaction between the water surface and the rising gas bubble, which pushes the surface layer into motion.

2. Layout of Experimental Points and Measurement Method

2.1. Pressure Measurement

Over a long period of time, progress in explosion wave-making research has been slow, primarily because of measurement techniques. To this end, we selected a low-frequency pressure transducer that has a wide measurement range. Its output signal is amplified by a low-frequency charger amplifier before reaching a MR-30 tape recorder. Finally, the tape is played on a 545/c computer for processing. This kind of wide-range pressure transducer can withstand the shock wave without damage. Moreover, the low-frequency response of the measurement system can effectively suppress the shock-wave signal in water. Our experience proves that this system has the capability to record the wave pressure near the explosion region.

Based on the Lagrange equation for a non-viscous fluid, the pressure P at any point in the field can be expressed as follows:

$$P = -\frac{1}{2}\rho U^2 - \rho g z - \rho \frac{\partial \phi}{\partial t}$$

The second term on the right is the hydrostatic pressure. The first and third terms are the hydrodynamic pressure generated by velocity and unsteady motion, respectively. When the sensing face of the pressure transducer is perpendicular to the flow, the velocity drops to zero because the flow is interrupted. The pressure thus measured should be the total pressure. However, because the recorder is zeroed at the hydrostatic pressure level before the experiment, the instrument actually records the difference between the total pressure and the hydrostatic pressure. When the sensing face of the transducer is parallel to the flow, the flow velocity no longer plays a role. The instrument should record the actual pressure at the point of measurement undisturbed by the flow field.

2.2. Wave Measurement

Tantalum wire capacitor transducers were installed at various measurement points. These points were secured on rods to measure the waves generated by the explosion.

3. Results and Discussion

3.1. Wave Pressure

Experimentally, the data shows that (1) the wave pressure drops off rapidly with distance. Its primary range of influence is near the center of explosion. (2) The pressure measured by a transducer facing the flow is greater than that parallel to the flow. (3) There is a maximum wave pressure near the surface; it then decreases with depth and then rises slightly after reaching a certain depth. Its effective depth is approximately equivalent to the crater. The data is shown in Tables 1 and 2.

3.2. Wave Height and Period

Based on over a hundred wave curves recorded by the wave height instrument at different places, the wave generated by explosion bears the characteristics of non-linear gravity waves.

3.2.1. Wave Height

It was experimentally found that (i) the product of wave height and distance remains more or less constant for a given amount of explosive and specific height. This is in agreement with experimental results obtained abroad with chemical and nuclear explosives.[2] (ii) At a fixed

Table 1. Measured Wave Pressure (depth = 0.05 m)

W(g)	$\bar{H}$(cm/kg$^{\frac{1}{3}}$)	R(m), P(1 × 10^{4}Pa)				
500	0	R	3.33	4.46	5.75	5.75*
		P	16.95	2.85	2.29	1.75
500	20	R	3.03	4.09	5.20	5.20
		P	20.0	2.75	2.16	0.72
300	0	R	3.03	4.09	5.20	5.20
		P	6.90	1.38	1.22	0.92
300	0	R	2.98	4.13	5.00	5.00
		P	1.90	/	0.97	0.60
300	20	R	3.03	4.09	5.20	5.20
		P	1.44	1.97	1.71	0.57
100	0	R	3.03	4.09	5.20	5.20
		P	5.50	1.64	/	/
100	0	R	2.98	4.13	5.00	5.00
		P	0.96	0.91	0.98	0.11
100	20	R	3.03	4.09	5.20	5.20
		P	6.20	/	/	/

Note: The last column was obtained with the sensing surface facing up.

Table 2. Measured Wave Pressure at Different Depths (10^4 Pa) ($\bar{H}$=0)

R(m)		2.60				2.83			
h(m)		+0.05	−0.01	−0.15	−0.45	+0.05	−0.15	−0.25	−0.45
P	W = 500g	0	9.17	1.19	2.05	2.93	3.39	1.85	2.09
	W = 300g					1.18	1.17	0.68	1.10

Note: As far as wave pressure versus depth is concerned, there is a pressure maximum near the water surface (i.e., -0.01, -0.05 m). Down to -0.45 m, there seems to be another peak.

distance, the wave height decreases with increasing specific height. At the same specific height and distance, the wave height increases with the amount of explosive used. The following equation is derived from regression of experimental data:

$$H = 116.2 \frac{W^{0.4616}}{R} e^{-0.02552\bar{H}}$$

When $\bar{H} = 0$ or 20 (cm/kg$^{1/3}$), the calculated values are in very good agreement with measured values.

3.2.2. Wave Height and Explosion Depth

Based on an earlier study,[3] when an explosion takes place underwater, the surface wave height is dependent upon the explosion depth (see Figure 2). There are two peaks. The upper critical depth zone is approximately equivalent to half a charge depth. The lower critical depth is approximately eight times the radius of the explosive charge. In order to verify this phenomenon, we picked four explosion depths: 0.5 R_0, 4 R_0, 8 R_0 and 10 R_0 (R_0 is the radius of the explosive charge). The transducers were placed above the water surface. The specific distances between points of measurement and the explosion center are 3.3, 4.48 and 6.0 (m/kg$^{1/3}$). The results show that the upper critical depth is approximately between 0.5 R_0 and 4 R_0 and the lower critical depth is at 10 R_0.

3.2.3. Wave Period and Velocity

The wave period increases with the amount of explosive charge and decreases with increasing specific height. When $\bar{H}$ = 0-20, W = 1-16 (kg), the wave period at R = 16 m is approximately 1.9-2.6 seconds. The mean wave velocity at this time is 2.1-2.6 seconds.

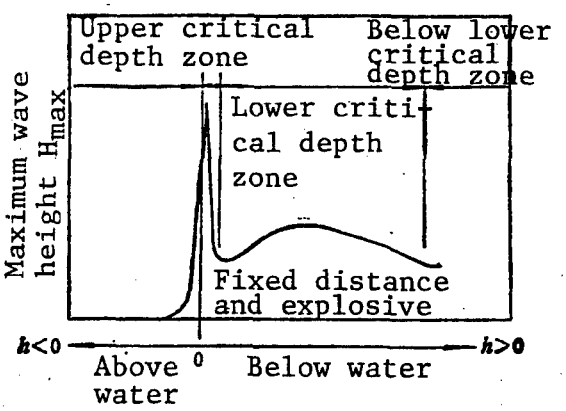

Figure 2. Wave Height vs. Explosion Depth

3.2.4. Wave Reflection

The reflection index of the wave generated by explosion upon encountering an obstacle was measured to be 1.6.

The authors wish to acknowledge the support of Institute 702 of China State Shipbuilding Corporation and the Naval Chemical Defense Institute.

References

1. J. Flores and M. Holt, "Shock-Wave Interactions With the Ocean Surface," PHYS. FLUIDS, 25(2), February (1982).

2. Gregory K. Hartmann, "Wave-Making by an Underwater Explosion," AD-AO38276, September (1976).

3. Maurice Holt, "Underwater Explosions Ann," REV. FLUID MECH., 9 (1977), 187-214.

Foreign Broadcast Information Service (FBIS) and Joint Publications Research Service (JPRS) publications contain political, military, economic, environmental, and sociological news, commentary, and other information, as well as scientific and technical data and reports. All information has been obtained from foreign radio and television broadcasts, news agency transmissions, newspapers, books, and periodicals. Items generally are processed from the first or best available sources. It should not be inferred that they have been disseminated only in the medium, in the language, or to the area indicated. Items from foreign language sources are translated; those from English-language sources are transcribed. Except for excluding certain diacritics, FBIS renders personal and place-names in accordance with the romanization systems approved for U.S. Government publications by the U.S. Board of Geographic Names.

Headlines, editorial reports, and material enclosed in brackets [ ] are supplied by FBIS/JPRS. Processing indicators such as [Text] or [Excerpts] in the first line of each item indicate how the information was processed from the original. Unfamiliar names rendered phonetically are enclosed in parentheses. Words or names preceded by a question mark and enclosed in parentheses were not clear from the original source but have been supplied as appropriate to the context. Other unattributed parenthetical notes within the body of an item originate with the source. Times within items are as given by the source. Passages in boldface or italics are as published.

SUBSCRIPTION/PROCUREMENT INFORMATION

The FBIS DAILY REPORT contains current news and information and is published Monday through Friday in eight volumes: China, East Europe, Soviet Union, East Asia, Near East & South Asia, Sub-Saharan Africa, Latin America, and West Europe. Supplements to the DAILY REPORTs may also be available periodically and will be distributed to regular DAILY REPORT subscribers. JPRS publications, which include approximately 50 regional, worldwide, and topical reports, generally contain less time-sensitive information and are published periodically.

Current DAILY REPORTs and JPRS publications are listed in *Government Reports Announcements* issued semimonthly by the National Technical Information Service (NTIS), 5285 Port Royal Road, Springfield, Virginia 22161 and the *Monthly Catalog of U.S. Government Publications* issued by the Superintendent of Documents, U.S. Government Printing Office, Washington, D.C. 20402.

The public may subscribe to either hardcover or microfiche versions of the DAILY REPORTs and JPRS publications through NTIS at the above address or by calling (703) 487-4630. Subscription rates will be provided by NTIS upon request. Subscriptions are available outside the United States from NTIS or appointed foreign dealers. New subscribers should expect a 30-day delay in receipt of the first issue.

U.S. Government offices may obtain subscriptions to the DAILY REPORTs or JPRS publications (hardcover or microfiche) at no charge through their sponsoring organizations. For additional information or assistance, call FBIS, (202) 338-6735,or write to P.O. Box 2604, Washington, D.C. 20013. Department of Defense consumers are required to submit requests through appropriate command validation channels to DIA, RTS-2C, Washington, D.C. 20301. (Telephone: (202) 373-3771, Autovon: 243-3771.)

Back issues or single copies of the DAILY REPORTs and JPRS publications are not available. Both the DAILY REPORTs and the JPRS publications are on file for public reference at the Library of Congress and at many Federal Depository Libraries. Reference copies may also be seen at many public and university libraries throughout the United States.